Likelihood-Based Modulation Classification for Multiple-Antenna Receivers

by

Ali Ramezani-Kebrya

A thesis submitted to the
Department of Electrical and Computer Engineering
in conformity with the requirements for
the degree of Master of Applied Science

Queen's University
Kingston, Ontario, Canada
September 2012

Abstract

Prior to signal demodulation, blind recognition of the modulation scheme of the received signal is an important task for intelligent radios in various commercial and military applications such as spectrum management, surveillance of broadcasting activities and adaptive transmission. Antenna arrays provide spatial diversity and increase channel capacity. This thesis focuses on the algorithms and performance analysis of the blind modulation classification (MC) for a multiple antenna receiver configuration.

For a single-input-multiple-output (SIMO) configuration with unknown channel amplitude, phase, and noise variance, we investigate likelihood-based algorithms for linear digital MC. The existing algorithms are presented and extended to SIMO. Using recently proposed blind estimates of the unknown parameters, a new algorithm is developed. In addition, two upper bounds on the classification performance of MC algorithms are provided. We derive the exact Cramér-Rao Lower Bounds (CRLBs) of joint estimates of the unknown parameters for one- and two-dimensional amplitude modulations. The asymptotic behaviors of the CRLBs are obtained for the high signal-to-noise-ratio (SNR) region. Numerical results demonstrate the accuracy of the CRLB expressions and confirm that the expressions in the literature are special

cases of our results. The classification performance of the proposed algorithm is compared with the existing algorithm and upper bounds. It is shown that the proposed algorithm outperforms the existing one significantly with reasonable computational complexity.

The proposed algorithm in this thesis can be used in modern intelligent radios equipped with multiple antenna receivers and the provided performance analysis, *i.e.,* the CRLB expressions, can be employed to design practical systems involving estimation of the unknown parameters and is not limited to MC.

Dedication

To my family

I am honored to have you.

Acknowledgments

First of all, I would like to express my deep gratitude to my supervisor, Professor Il-Min Kim for his constant support and precious suggestions. Without his encouragement and motivation, this work would not have been possible. I would like to thank Professor François Chan for his guidance, support, and valuable comments.

My special thanks go to Mr. Saeed Akhavan Astaneh for our discussions and his insightful guidance. I would like to thank all of my colleagues at the *Wireless Information Transmission Lab*, in particular Dr. Yang, Dr. Jeong, Peng, Mohammad, Yaser, and Andrew. Thank you to my friends Shahab, Mostafa, Hossein, and Milad. Without them, my life in Kingston could not have been full of fun and joy.

Last but not least, I would like to express my deepest gratitude to my great parents for their unconditional love, supportive encouragement, and endless selflessness throughout my life. I am indebted to them forever. I am thankful to my sister Maryam and my brother Hamid-Reza for their support. Although they are living far from me, their words of encouragement and warm support gave me the motivation to complete this thesis.

Table of Contents

List of Tables

List of Figures

Chapter 1

Introduction

1.1 Modulation Classification

Automatic modulation classification (MC) is to recognize the unknown modulation scheme of the received signal. Identifying the modulation type is an important step before the demodulation at the receiver side of both military and commercial communication systems. Fast growth of commercial wireless systems demands efficient spectrum access algorithms that are adaptive to the environment. Software defined radio (SDR) is an example of civilian adaptive systems. For military applications, it is desirable to have a reliable and secure communication in a crowded spectrum shared with many jamming signals. In practice, due to lack of knowledge about multiple unknown parameters such as the symbol duration, carrier frequency/phase offsets, noise variance, channel amplitude, and so on, MC becomes more difficult. In wireless environments, the problem is even more challenging because of multi-path fading, frequency selective and time-varying channels. In order to reduce the overhead, blind techniques that do not rely on the training symbols can be employed to

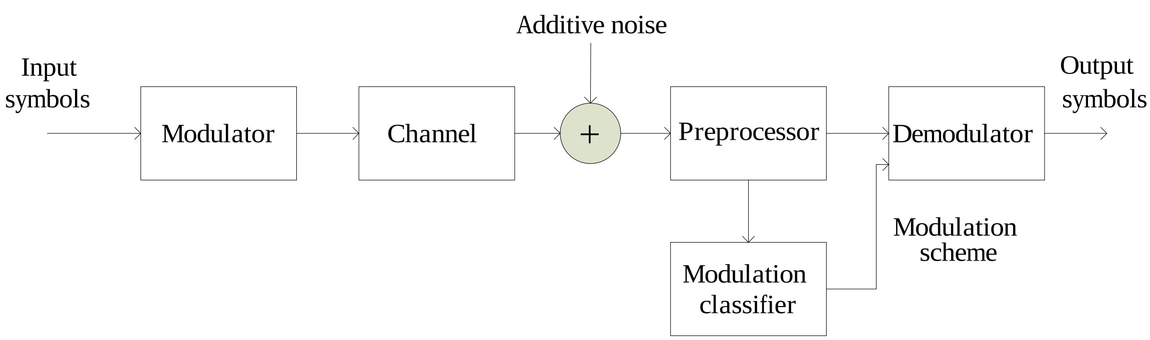

Figure 1.1: Block diagram of a system employing modulation classification.

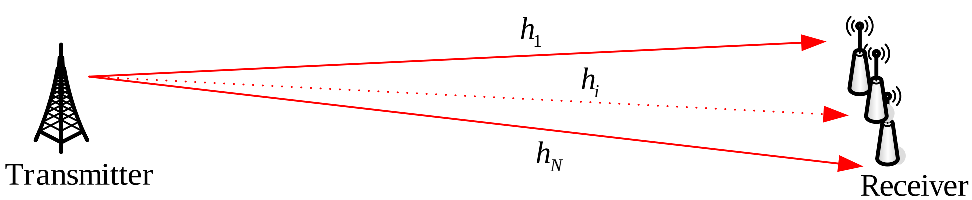

Figure 1.2: Single-input-multiple-output configuration.

estimate the unknown parameters. In Fig. 1.1, the block diagram of a typical system employing MC algorithms is shown. Estimation of the symbol duration, channel amplitude/phase, noise reduction, waveform recovery, and equalization are included in the signal preprocessing task. Signal demodulation and detection of the information-bearing symbols are performed after the modulation scheme is recognized.

In order to improve the system performance and combat the fading effects of the environment, multiple antennas can be employed at the receiver side as demonstrated in Fig. 1.2. An independent signal path is provided from the transmitter to each receiver antenna such that multiple independent replicas of the input symbol are obtained at the receiver side. The provided spatial diversity improves the reliability of the communication system.

The two general classes of automatic MC algorithms are likelihood-based (LB) and feature-based (FB). The decision is made based on the likelihood function (LF) of the received signal in the former. The latter recognizes the modulation type employing the observed values of some features of the received signal. FB approaches, yet suboptimal, usually lead to lower computational complexity.

In practice, a classifier that identifies the modulation scheme of the received signal in a short observation period with a high probability of correct classification is of interest. Furthermore, it is desirable to classify many types of modulation schemes for the case of multiple unknown parameters with reasonably low computational complexity.

1.1.1 Likelihood-based approaches

Using LB approaches, the LF of the received signal given each modulation type is computed and further compared in order to recognize the modulation scheme. The transmitted symbols and many parameters such as channel amplitude, phase, and noise variance are assumed to be unknown. In order to derive unconditional LFs with respect to the unknown quantities, *i.e.,* unknown symbols and parameters, one can take expectation or use proper estimates. Based on the approach employed to compute unconditional LFs, LB-MC algorithms are categorized into four groups. Average Likelihood Ratio Test (ALRT) [1, 2, 3, 4, 5, 6, 7], Generalized Likelihood Ratio Test (GLRT) [8, 1, 2], Hybrid Likelihood Ratio Test (HLRT) [6, 1, 7, 5, 2, 8] and Quasi Hybrid Likelihood Ratio Test (QHLRT) [5, 6, 7, 2] are the well-known LB algorithms developed in the literature that we now briefly discuss.

ALRT

Using ALRT, the unknown quantities are supposed to be random variables with known probability density/mass functions (PDFs/PMFs). Let H_m denote the hypothesis that the m-th modulation scheme is used for $m = 1, \cdots, N_{\text{mod}}$, where N_{mod} indicates the number of modulation candidates. The LF of the received signal under H_m is given by

$$\text{LF}_{\text{ALRT}}(\boldsymbol{r}|H_m) = \mathbb{E}_{\boldsymbol{\nu}_m}\left[\text{LF}(\boldsymbol{r}|\boldsymbol{\nu}_m, H_m)\right], \tag{1.1}$$

where $\boldsymbol{r}$ denotes the column vector of observed signals and $\boldsymbol{\nu}_m$ is the column vector of unknown quantities. In order to derive (1.1), one requires the conditional PDF of the unknown quantities, *i.e.,* $f(\boldsymbol{\nu}_m|H_m)$. However, this information is not necessarily available in practice.

GLRT

One can consider the unknown quantities as unknown deterministic yielding the GLRT algorithm. Although a uniformly most powerful (UMP) test leads to the optimum algorithm [22], it does not necessarily exist. One can use the maximum likelihood estimates (MLEs) of the unknown quantities leading to GLRT where the LF under H_m is given by

$$\mathrm{LF}_{\mathrm{GLRT}}(\boldsymbol{r}|H_m) = \max\nolimits_{\boldsymbol{\nu}_m} \mathrm{LF}(\boldsymbol{r}|\boldsymbol{\nu}_m, H_m), \tag{1.2}$$

The GLRT algorithm fails to classify the nested constellations, *e.g.,* binary phase-shift keying (BPSK) and quadrature phase-shift keying (QPSK) since maximization over the unknown symbols can yield the same values of LFs for the nested constellations [10].

HLRT

As a combination of ALRT and GLRT, one can take expectation over some unknown quantities while employing proper estimates for the others. Taking expectation over the unknown symbols, the problem of nested constellations is resolved [1]. The LF under H_m is expressed as,

$$\mathrm{LF}_{\mathrm{HLRT}}(\boldsymbol{r}|H_m) = \mathbb{E}_{\boldsymbol{\nu}_{m,1}} \left[\mathrm{LF}(\boldsymbol{r}|\boldsymbol{\nu}_{m,1}, \hat{\boldsymbol{\nu}}_{m,2}, H_m) \right], \tag{1.3}$$

where $\boldsymbol{\nu}_m = [\boldsymbol{\nu}_{m,1}^\dagger \;\; \boldsymbol{\nu}_{m,2}^\dagger]^\dagger$ and † denotes the transpose operation. It is usual to take $\boldsymbol{\nu}_{m,1}$ and $\boldsymbol{\nu}_{m,2}$ as the unknown parameters and transmitted symbols respectively. When the MLEs are employed to obtain $\hat{\boldsymbol{\nu}}_{m,2}$ in (1.3), the resulting algorithm is referred to as HLRT. The problem with HLRT is very high computational complexity [7] which makes it impractical.

	$\boldsymbol{\nu}_{m,2}$	$\boldsymbol{\nu}_{m,1}$
ALRT	Taking expectation	Taking expectation
GLRT	Employing MLE	Employing MLE
HLRT	Employing MLE	Taking expectation
QHLRT	Employing non-MLE	Taking expectation

Table 1.1: Likelihood-based algorithms

QHLRT

As an alternative to HLRT, one can use the proper non-data-aided (NDA) non-MLEs to derive $\hat{\boldsymbol{\nu}}_{m,2}$ in (1.3) and the algorithm is referred to as QHLRT. Using the method of moments (MoM) to estimate $\boldsymbol{\nu}_{m,2}$, it was demonstrated in [7] that QHLRT-MoM yields similar performance to HLRT although QHLRT-MoM is substantially simpler to implement. Hence, the QHLRT-MoM algorithm could be a promising algorithm for the scenarios where there are many unknown parameters.

Table 1.1 summarizes different LB algorithms for MC.

1.1.2 Feature-based approaches

In the literature, many features of the received signal were used for MC such as the variance of the central normalized signal amplitude, phase and frequency [23], the variance of the zero-crossing interval [24], the variance of the magnitude of the signal wavelet transform [25, 26, 27], and moments/cumulants/cyclic cumulants of the received signal [28, 29, 30, 31, 13]. Fuzzy logic [32] and shape recovery of the constellation [33] are also examples of FB approaches. Using the FB algorithms, the modulation type, *i.e.,* pulse/amplitude modulation (PAM/QAM), frequency/phase shift keying (FSK/PSK), is first recognized and then the number of constellation points is estimated. In order to make a decision, a binary tree structure is usually used where a proper statistic corresponding to a modulation scheme is compared against a threshold at each node. As an example, one can consider a straightforward feature, the instantaneous amplitude, phase, and frequency. While the instantaneous amplitude is constant for PSK and FSK signals, it fluctuates for PAM and QAM. The information is in the instantaneous carrier phase and frequency for PSK and FSK respectively.

1.2 Estimation and Performance Measure

In this section, we briefly discuss fundamental background concepts of point estimation.

Let $\boldsymbol{x} = [x_1 \cdots x_n]^\dagger$ denote the column vector of the observed data drawn independently and identically distributed (i.i.d) from a member of a class of probability models $p_\theta(\boldsymbol{x})$, where θ is some parameter. The parameter space and data space are denoted by Ψ and $\mathcal{X}$ respectively. A function $\xi(\cdot)$ from $\mathcal{X}$ onto Ψ is called an estimator and a realization of the estimator, $\xi(\boldsymbol{x})$ is called the estimate. Notations $\xi(\boldsymbol{x})$ and $\hat{\theta}$ are used interchangeably in the following.

In order to evaluate the performance of any estimator, two important functions are bias and Mean Square Error (MSE). The bias of an estimator is defined by

$$\begin{aligned} \mathrm{B}_\xi(\theta) &= \mathbb{E}_\theta(\hat{\theta} - \theta) \\ &= \int_{-\infty}^{\infty} \cdots \int_{-\infty}^{\infty} p_\theta(\boldsymbol{x})(\hat{\theta}(\boldsymbol{x}) - \theta)\mathrm{d}\boldsymbol{x}, \end{aligned} \tag{1.4}$$

where $\mathbb{E}_\theta$ denotes expectation over the conditional distribution of the data given θ.

Let $\mathrm{Var}_\xi(\theta)$ denote the variance of the estimator. MSE is expressed as

$$\mathrm{MSE}_\xi(\theta) = \mathbb{E}_\theta\left((\hat{\theta} - \theta)^2\right) = \mathrm{B}_\xi^2(\theta) + \mathrm{Var}_\xi(\theta). \tag{1.5}$$

An estimator $\tilde{\xi}$ will be referred to as a minimum variance unbiased estimator (MVUE) if it achieves the minimum variance among the class of unbiased estimators, *i.e.,* the estimators with $\mathrm{B}_\xi(\theta) = 0$ for all θ. In practice, however, a MVUE might not exist or demand a huge complexity which is not of interest for real-time applications.

1.2.1 MLE

Intuitively, it is desirable to have an estimator under which the observed data is most likely, *i.e.,* the LF of the data is maximized. The MLE is important because it is applicable to any class of probability model with arbitrary set of parameters. Mathematically, given the observation data $\boldsymbol{x}$, the MLE is given by

$$\hat{\theta}_{\mathrm{ML}} = \arg\max_{\theta \in \Psi} \; p_\theta(\boldsymbol{x}). \tag{1.6}$$

Denoting by $\omega(\theta)$ the prior distribution of the parameter, the posterior distribution is given by

$$\omega(\theta|\boldsymbol{x}) = \frac{\omega(\theta) p_\theta(\boldsymbol{x})}{\int_\Psi \omega(\theta) p_\theta(\boldsymbol{x}) \mathrm{d}\theta}. \tag{1.7}$$

If the priori $\omega(\theta)$ is assumed to be uniformly distributed, the maximization of the LF will be the same as the maximization of the posteriori in (1.7). For i.i.d. data, it is easier to take logarithm since it leads to working with summations and not multiplications. The expression of the MLE when the log-likelihood function (LLF) is maximized is obtained by

$$\hat{\theta}_{\mathrm{ML}} = \arg\max_{\theta \in \Psi} \sum_{i=1}^{n} \log p_\theta(x_i). \tag{1.8}$$

In general, the two well-known types of estimates in wireless communications are data-aided (DA) and non-data-aided (NDA) estimates.

1.2.2 Data-aided estimates

If transmitted data such as training symbols are employed to facilitate the estimation of the unknown parameters, the estimation approach is called DA. The DA MLE for the unknown signal-to-noise-ratio (SNR) is used in [15]. In [34], an algorithm for DA carrier frequency estimation for the case of burst PSK signals is proposed.

1.2.3 Non-data-aided estimates

Although DA algorithms provide more accurate estimates, they impose a high burden on the receiver. In order to reduce signaling overhead and boost the throughput of the system, NDA estimates can be used. Furthermore, employing blind approaches might be inevitable in some practical scenarios such as military applications. NDA estimates for the unknown SNR and symbol rate are studied in [35, 15, 18] and in [36] respectively.

The expressions of theoretical performance analysis are useful tools for designing practical systems. If deriving the exact theoretical performance analysis is not tractable, one can resort to theoretical bounds on the performance. For the practical scenarios involving estimation of the unknown parameters, some system designing parameters can be obtained by minimizing the derived expressions of bounds on the performance analysis, *e.g.,* the Cramér-Rao Lower Bounds (CRLBs).

1.2.4 Cramér-Rao Lower Bound

Lower bounds on the variance of estimators of the unknown parameters are given by the CRLB. Among unbiased estimators, an estimator achieving this bound is efficient in terms of minimizing MSE. However, there might be no estimator achieving the CRLB in practice.

Let $\boldsymbol{\theta} = [\theta_1, \cdots, \theta_K]^\dagger$ denote a K dimensional parameter vector. The Fisher information matrix (FIM) is defined as $\mathrm{I}(\boldsymbol{\theta}) = [\mathrm{I}_{i,j}(\boldsymbol{\theta})]$ for $i, j = 1, \cdots K$, where

$$\mathrm{I}_{i,j}(\boldsymbol{\theta}) = \mathrm{Cov}_{\boldsymbol{\theta}}(\frac{\partial}{\partial\theta_i}\log p_{\boldsymbol{\theta}}(\boldsymbol{x}), \frac{\partial}{\partial\theta_j}\log p_{\boldsymbol{\theta}}(\boldsymbol{x})). \tag{1.9}$$

The following regularity conditions should hold in order to use (1.9) for deriving the CRLB

- The FIM is always defined, *i.e.*, $\frac{\partial}{\partial\theta_i}\log p_{\boldsymbol{\theta}}(\boldsymbol{x})$ exists for all $\boldsymbol{x}$ and $i = 1, \cdots, K$.
- The integration and differentiation operations can be interchanged in $\frac{\partial}{\partial\theta_i}\int p_{\boldsymbol{\theta}}(\boldsymbol{x})\mathrm{d}\boldsymbol{x}$ for $i = 1, \cdots, K$.
- The support of $p_{\boldsymbol{\theta}}(\boldsymbol{x})$ does not depend on $\boldsymbol{\theta}$.

It is demonstrated that the FIM can be expressed as [37]

$$\mathrm{I}_{i,j}(\boldsymbol{\theta}) = -\mathbb{E}_{\boldsymbol{\theta}}\left[\frac{\partial^2}{\partial\theta_i\partial\theta_j}\log p_{\boldsymbol{\theta}}(\boldsymbol{x})\right]. \tag{1.10}$$

One-dimensional parameter

Assuming $K = 1$, the lower bound on the variance of any estimator of θ, *e.g.*, $\xi(\boldsymbol{x})$, is given by [37]

$$\mathrm{Var}_\xi(\theta) \geq \frac{(1 + \frac{\mathrm{d}}{\mathrm{d}\theta}\mathrm{B}_\xi(\theta))^2}{\mathrm{I}(\theta)}, \tag{1.11}$$

where $\mathrm{I}(\theta) = -\mathbb{E}_\theta\left[\frac{\mathrm{d}^2}{\mathrm{d}\theta^2}\log p_\theta(\boldsymbol{x})\right]$. If $\tilde{\xi}$ is any unbiased estimator of θ, we will have $\mathrm{Var}_{\tilde{\xi}}(\theta) \geq 1/\mathrm{I}(\theta)$.

Multi-dimensional parameter

Assuming $\boldsymbol{\theta}$ is K-dimensional, the covariance matrix of any joint estimator of the unknown parameters satisfies [37]

$$\mathrm{Cov}_{\xi}(\boldsymbol{\theta}) \succeq \vartheta^\dagger(\boldsymbol{\theta})\mathrm{I}^{-1}(\boldsymbol{\theta})\vartheta(\boldsymbol{\theta}), \tag{1.12}$$

where $\vartheta(\boldsymbol{\theta}) = \left[\frac{\partial}{\partial\theta_1}\mathbb{E}_{\boldsymbol{\theta}}[\xi(\boldsymbol{x})], \cdots, \frac{\partial}{\partial\theta_K}\mathbb{E}_{\boldsymbol{\theta}}[\xi(\boldsymbol{x})]\right]^\dagger$ is the Jacobian matrix and $A \succeq B$ indicates that $A - B$ is a non negative definite matrix. Finally, for K-dimensional unbiased estimators, we have $\mathrm{Cov}_{\tilde{\xi}}(\boldsymbol{\theta}) \succeq \mathrm{I}^{-1}(\boldsymbol{\theta})$.

1.3 Motivation and Thesis Overview

Identifying the modulation scheme of the received signal is an important step before demodulation in various military and commercial applications. In particular, for the case of a multi-path fading environment when there are no available training symbols to form accurate channel state information (CSI) estimates, the problem becomes more challenging. Obtaining proper MC algorithms applicable to different propagation environments has attracted a lot of interest over the past two decades.

Using an array of antennas at the receiver side has turned out to boost the system performance and combat the fading effects of the environment. The spatial diversity provided by having multiple independent replicas of the transmitted symbol leads to capacity increase and probability of false detection decrease.

As a guide for system designers, the expressions of theoretical performance analysis are useful tools. For practical scenarios, optimizing the derived expressions of performance analysis, *e.g.,* minimizing the CRLBs of the unknown NDA parameter estimates, leads to maximizing the probability of correct classification. Hence, some optimum system parameters can be derived and then employed to orient the communication system design.

For a single-input-single-output (SISO) configuration, the problem of LB-MC was studied with unknown amplitude, noise variance and phase in [7] and for single-input-multiple-output (SIMO) configuration with unknown amplitude and phase in [5]. To the best of our knowledge, LB-MC for SIMO with unknown amplitude, phase, and noise variance has not been studied in the literature. This has motivated us to propose a new classification algorithm for SIMO with considering all the unknown parameters.

The expressions of the CRLBs of square QAM were derived in [19] and [20] for the unknown SNR and phase respectively. In [7], the CRLBs of NDA joint estimates of the unknown signal amplitude, phase, and noise variance were derived for BPSK and QPSK. Those results cannot be directly extended to the general rectangular QAM. This has motivated us to analyze the CRLBs of the unknown amplitude, phase, noise variance, and SNR for general rectangular $I \times J$-QAM.

The remainder of this thesis is organized as follows. In Chapter 2, we study the problem of LB-MC for a SIMO configuration with unknown amplitude, phase, and noise variance. A new LB algorithm is proposed using the state-of-the-art estimates for the unknown parameters. Furthermore, the expressions of the CRLBs of the unknown amplitude, phase, noise variance, and SNR for rectangular QAM are derived. It is demonstrated that the results available in the literature are special cases of our results. Finally, we draw the conclusions of this thesis in Chapter 3.

1.4 Thesis Contributions

This thesis aims to study the problem of MC for a SIMO configuration and analyze the CRLBs for a general rectangular QAM constellation. The main contributions of the thesis are summarized as follows:

- A new LB-MC algorithm assuming unknown amplitude, phase, and noise variance is proposed. We first obtain the conditional LFs of the received signal under the modulation scheme and unknown quantities. Then we find the unconditional LFs of the received signal by using the state-of-the-art NDA estimates for the unknown parameters and taking expectation over the transmitted symbols. We propose a weighted sum (WS)-based algorithm for a SIMO configuration, and show that our proposed algorithm outperforms the extended algorithm proposed in [5]. Furthermore, an upper bound on the performance of any MC algorithm and another bound on the QHLRT-based algorithms are provided. The former, referred to as ALRT-upper bound (ALRT-UB), is derived to evaluate the performance degradation of the MC algorithms when compared to the ideal case, where there is no unknown parameter. The latter, referred to as QHLRT-UB, provides a bound on QHLRT-based algorithms employing NDA and unbiased estimates of the unknown parameters. Numerical results demonstrate that the classification performance of the proposed algorithm is close to the upper bounds and is significantly better than the existing work.

- We obtain exact expressions of the CRLBs of amplitude, phase, noise variance, and SNR for general rectangular $I \times J$-QAM signals and demonstrate that the results available in the literature are special cases of our results. Furthermore, we obtain asymptotic CRLBs for the high SNR regime. Numerical results show the accuracy of our analysis.

Chapter 2

Modulation Classification for Multiple-Antenna Receivers

We consider a single-input-multiple-output (SIMO) configuration with channel amplitude, phase, and noise variance as the unknown parameters. We investigate likelihood-based (LB) algorithms for linear digital modulation classification (MC). The existing MC algorithms are extended to the case of SIMO. We propose a new Quasi Hybrid Likelihood Ratio Test (QHLRT) algorithm using the state-of-the-art non-data-aided (NDA) estimates of the unknown parameters. Furthermore, an upper bound on the classification performance of any MC algorithm and a tighter upper bound on the performance of QHLRT algorithms are obtained. The exact Cramér-Rao Lower Bound (CRLB) expressions of NDA joint estimates of the unknown parameters are also presented for one- and two-dimensional amplitude modulations, *i.e.,* PAM and QAM. The asymptotic behaviors of the CRLBs are obtained for the high signal-to-noise-ratio (SNR) regime. Numerical results demonstrate the accuracy of the CRLB expressions and verify that the expressions available in the literature are special cases of our results. The classification performance of the proposed algorithm is compared with the upper bounds and the existing QHLRT which is based on the method of moments (MoM). It is shown that our proposed algorithm outperforms the QHLRT-MoM algorithm significantly with reasonable computational complexity.

2.1 Introduction

The automatic (blind) modulation classification (MC) is to determine the unknown modulation type of the received signal and it is an important task of intelligent radios, which are able to sense and adapt to the environment, such as in various civilian and military applications. In the case of fading environments, the problem becomes more challenging as there are multiple unknown parameters that should be known or estimated before we can find the modulation scheme. From a system viewpoint, modulation classifiers consist of two steps: signal preprocessing and a proper classification algorithm. The signal preprocessing step may include estimation of signal carrier frequency, phase, amplitude, noise variance, waveform recovery, and symbol interval. Depending on the assumptions about prior knowledge of signal parameters, which can be their estimates or only their distributions, different preprocessing tasks with corresponding accuracy levels are needed.

The two general classes of MC are likelihood-based (LB) and statistical pattern recognition-based known as feature-based (FB). The former is based on the likelihood function tests of the received signal[1, 2, 3, 4, 5, 6, 7, 8, 9, 10], while the latter is based on the features of the received signal [1, 11, 12, 13]. Many LB algorithms have been investigated in the literature such as Average Likelihood Ratio Test (ALRT) [1, 2, 3, 4, 5, 6, 7], Generalized Likelihood Ratio Test (GLRT) [8, 1, 2], and Hybrid

Likelihood Ratio Test (HLRT) [6, 1, 7, 5, 2, 8]. To perform ALRT, one needs to have a priori knowledge about the actual distributions of the unknown parameters, *i.e.*, channel amplitude, phase, and noise variance; otherwise it does not lead to the maximum probability of correct classification. In addition to having many unknown parameters, ALRT suffers from very high computational complexity [4, 5, 6, 7, 2]. Another LB algorithm is GLRT where one computes the probability density function (PDF) of the received signal by employing maximum likelihood estimates (MLE) of unknown quantities (*e.g.,* transmitted symbols, channel amplitude, phase, and noise variance). However, GLRT fails to identify the nested signal constellations correctly, such as 16-QAM and 64-QAM, as this approach can lead to the same value of the likelihood function (LF) [10]. To address the nested constellations problem of GLRT, one can use HLRT that is a hybrid of ALRT and GLRT. With using HLRT, one takes the average over all possible combinations of the symbol sequence in calculating the PDF of the received signal, employing the MLE of the unknown parameters in lieu of taking expectation. In fact, one can consider channel amplitude, phase and noise variance as unknown deterministics, and symbols as random variables with known probability mass function (PMF). One can use MLE regardless of prior probability of the corresponding parameter. Because HLRT as well as ALRT involves performing an exhaustive search over the LFs, a less complex classifier is desirable. With the Quasi Hybrid Likelihood Ratio Test (QHLRT), non-data-aided (NDA) non-MLEs of the unknown parameters is used to calculate the LFs, and thus, the computational complexity reduces significantly [5, 6, 7, 2].

In [9], an LB-MC algorithm for wireless sensor networks was studied with uniformly distributed unknown carrier phase, where local decisions are sent to the sensor network centre to perform a decision fusion algorithm. An FB-MC method based on higher-order statistics (HOS) algorithm was proposed in [11]. The authors of [12] have analyzed a fourth order cumulant based multiuser MC for a multi-path fading environment. In [5], an LB-MC algorithm was proposed for a *multiple* antenna configuration with unknown phase and amplitude. Because the NDA parameter estimates used in [5] are conventional ones which are not accurate enough, [17] and [18] have proposed new NDA estimates for phase and amplitude recovery, respectively, which outperform the conventional ones significantly. To the best of our knowledge, LB-MC for SIMO with unknown amplitude, phase, and noise variance has not been studied in the literature. In addition, the recently proposed NDA estimates have not been applied to MC yet. It is desirable to develop a new LB-MC for multiple antenna configuration based on the state-of-the-art parameter estimates with amplitude, phase, and noise variance as the unknown parameters.

In this chapter, we propose a new LB-MC algorithm considering amplitude, phase, and noise variance to be unknown for a multiple antenna scenario. Specifically, we first find the conditional LFs of the received signal given the modulation scheme and unknown quantities. Then we compute the unconditional LFs of the received signal by averaging over symbols and employing appropriate estimates for the unknown parameters. Using the obtained LFs, we propose a weighted sum (WS)-based algorithm to perform blind MC, and show that our algorithm outperforms the one proposed in [5]. Furthermore, two upper bounds on the performance of any MC algorithms and QHRLT-based algorithms are proposed. The former, the ALRT-upper bound (ALRT-UB), is obtained to observe the performance loss of MC algorithms when compared to the ideal case, *i.e.*, no unknown parameter. The latter, which is referred to as QHLRT-UB, provides a bound for QHLRT-based algorithms employing NDA and unbiased estimates of the unknown parameters. It is well-known that the Cramér-Rao Lower Bounds (CRLBs) give the lower bounds on the variances of joint estimates of some unknown parameters. In other words, an upper bound on the performance of QHLRT-based MC algorithms, *i.e.*, lower bound on the classification error, is determined using the CRLBs as the variances of the unknown parameter estimates. In [7, 20, 19], the CRLBs of NDA joint estimates of the unknown parameters were derived for binary phase-shift keying (BPSK), quadrature phase-shift keying (QPSK), and square quadrature amplitude modulation (QAM). We obtain the CRLBs for general rectangular $I \times J$-QAM signals and show the derivations in the literature are special cases of our derived results. Also, we derive the asymptotic CRLBs for high signal-to-noise-ratio (SNR) range. Numerical results demonstrate the merit of using our proposed MC algorithm and the accuracy of our analysis.

The rest of this chapter is organized as follows: The system model is described in Section 2.2. Extending the existing algorithms to the case of multiple antennas is presented in Section 2.3. Our new WS-based MC algorithm is proposed in Section 2.3. In Section 2.4, we derive the CRLBs of the unknown parameters for rectangular $I \times J$-QAM signals, and we show the results reported in [7, 19, 20] are special cases of our results. Using the derived CRLBs, an upper bound on the performance of QHLRT-based algorithms is obtained. Numerical results for the CRLBs are presented in Section 2.5. We also compare the performance of the proposed WS-based and existing QHLRT-based algorithms with ALRT-UB and QHLRT-UB. Conclusions are drawn in Section 2.6.

Notation: We use $A := B$ to denote that A, by definition, equals B. For a complex number C, $|C|$ and $\sphericalangle C$ indicate the norm and phase of C. In order to represent the transpose and Hermitian transpose of vector $\boldsymbol{\nu}$, we use $\boldsymbol{\nu}^\dagger$ and $\boldsymbol{\nu}^H$ respectively. We use $\mathbb{E}[\cdot]$ to represent the expectation operation. Also, $z_1 \sim \mathcal{N}(\eta_1, \omega_1)$ indicates that z_1 is a real Gaussian random variable with mean η_1 and variance ω_1. Finally, $\boldsymbol{z}_2 \sim \mathcal{CN}(\boldsymbol{\eta}_2, \Omega_2)$ indicates that $\boldsymbol{z}_2$ is a circularly symmetric complex Gaussian (CSCG) random vector with mean $\boldsymbol{\eta}_2$ and covariance matrix Ω_2.

2.2 Problem Statement

Consider a single-input-multiple-output (SIMO) system with N receiving antennas. Our aim is to determine the unknown modulation type of the received signal. Let $\boldsymbol{s}^{(m)} := [s_1^{(m)}, \cdots, s_K^{(m)}]^\dagger$ denote the column vector of the transmitted symbols corresponding to the constellation $\mathcal{S}_m$ with $|\mathcal{S}_m| = M_m$ for $m = 1, \cdots, N_{\text{mod}}$, where N_{mod} denotes the number of modulation candidates. We use K to denote the number of samples of the received signals that we observe for MC. Let h_i denote the complex channel coefficient from the transmitter to the i-th receiving antenna. The problem of MC can be modeled as a multiple hypotheses testing problem. Modulation candidate m corresponds to the hypothesis H_m. Assuming the m-th hypothesis, the equivalent baseband signal at the receiver side is given by

$$\boldsymbol{r}_i = h_i \boldsymbol{s}^{(m)} + \boldsymbol{n}_i, \tag{2.1}$$

where $\boldsymbol{r}_i = [r_{i,1}, \cdots, r_{i,K}]^\dagger$ denotes the received signal sequence at the i-th receiving antenna and $\boldsymbol{n}_i = [n_{i,1}, \cdots, n_{i,K}]^\dagger$ is the additive white Gaussian noise (AWGN) with $\boldsymbol{n}_i \sim \mathcal{CN}(\mathbf{0}, \sigma_i^2 \mathbf{I}_K)$, where $\mathbf{I}_K$ represents a $K \times K$ identity matrix. We assume that the AWGN is spatially white, *i.e.*, $\mathbb{E}[\boldsymbol{n}_i^\dagger \boldsymbol{n}_l] = 0$ for $l \neq i$. It is assumed that $\{s_k^{(m)}\}_{k=1}^K$ are independently and uniformly distributed random variables over the signal constellation $\mathcal{S}_m$. We suppose that the channel coefficients $\{h_i\}_{i=1}^N$ and $\{\sigma_i^2\}_{i=1}^N$ are unknown at the receiver side since providing the training symbols to measure the instantaneous channel state information (CSI) perfectly for an unknown transmitter, *i.e.,* Data-Aided (DA) approach, either is impossible or causes a high burden to the destination. In order to have a practical system model, we assume a block fading environment where unknown channels are constant over the K observation time slots. Note that this is a common assumption for MC problems. Let $\boldsymbol{u}_i := [\alpha_i \; \varphi_i \; \sigma_i^2]^\dagger$ denote the vector of the unknown parameters, where α_i and φ_i represent unknown channel amplitude and phase of the i-th channel respectively. From a Bayesian view point, the maximum a posterior probability (MAP) test leads to the optimum classifier. Here, we assume equi-probable modulation candidates, which reduces the optimum classifier to ML. In other words, modulation m is selected if the LF of the received signal given H_m is larger than for the other hypotheses. Given the transmitted symbols $\boldsymbol{s}^{(m)}$ and the unknown parameter vectors, the LF under the m-th hypothesis is given by

$$f(\{\boldsymbol{r}_i\}_{i=1}^N | \boldsymbol{s}^{(m)}, \{\boldsymbol{u}_i\}_{i=1}^N, H_m) = \prod_{k=1}^K \prod_{i=1}^N \mathcal{R}_{i,k}^{(m)}, \tag{2.2}$$

where

$$\mathcal{R}_{i,k}^{(m)} = \left(\pi\sigma_i^2\right)^{-1} \exp\left(-\frac{|r_{i,k} - \alpha_i e^{j\varphi_i} s_k^{(m)}|^2}{\sigma_i^2}\right). \tag{2.3}$$

In (2.2), transmitted symbols and parameter vectors are unknown. That is, we should take expectation or use appropriate estimates to have unconditional LFs (LFs under each hypothesis are of interest). Note that taking expectation with respect to the parameter vectors gives the optimal Bayes' test; however, it requires additional information about the PDF of channels and noise variance which is not necessarily available. With the LFs calculated under all the hypotheses, the joint ML decision is made to find the modulation scheme, *i.e.*,

$$\hat{m} = \arg \max_{m \in \{1,\cdots,N_{\text{mod}}\}} \log\left(f(\{\boldsymbol{r}_i\}_{i=1}^N | H_m)\right), \tag{2.4}$$

where $\hat{m}$ is the estimate of the modulation.

2.3 MC for Multiple Antennas

2.3.1 Simple Extension of the Existing Algorithms

The problem of LB-MC has been studied for a single-input-single-output (SISO) configuration with unknown amplitude, noise variance, and phase in [7]; and for SIMO configuration with unknown amplitude and phase in [5]. To the best of our knowledge, LB-MC for SIMO with unknown amplitude, phase, and noise variance has not been studied in the literature. In this section, by extending the results reported in [7, 5], it is possible to come up with MC algorithms for SIMO configuration with unknown amplitude, phase, and noise variance. Note that these expressions presented in this section have not been explicitly reported in the literature, although it is not difficult to derive them.

ALRT

With using ALRT, the PDF of $\{\boldsymbol{r}_i\}_{i=1}^N$ conditioned on H_m for $m = 1, \cdots, N_{\text{mod}}$ is obtained by averaging (2.2) over the unknown symbols and parameter vectors, which can be expressed as

$$f_{\text{ALRT}}(\{\boldsymbol{r}_i\}_{i=1}^N | H_m) = \mathbb{E}_{\boldsymbol{s}^{(m)}} \mathbb{E}_{\{\boldsymbol{u}_i\}_{i=1}^N} \left[f(\{\boldsymbol{r}_i\}_{i=1}^N | \boldsymbol{s}^{(m)}, \{\boldsymbol{u}_i\}_{i=1}^N, H_m) \right]. \tag{2.5}$$

Since $\{\boldsymbol{u}_i\}_{i=1}^N$ are independent random vectors, the expectation can be written as $\mathbb{E}_{\boldsymbol{s}^{(m)}}\mathbb{E}_{\boldsymbol{u}_1}\cdots\mathbb{E}_{\boldsymbol{u}_N}[\cdot]$. However, obtaining the knowledge of the distributions of many unknown parameters requires a high signaling overhead. Since the information about the distributions of the parameter vectors is usually unavailable, ALRT is not of interest in practical scenarios. In the next subsections, two algorithms performing MC without having the knowledge of the distributions of the unknown parameters are presented.

HLRT

One can use appropriate estimates in lieu of taking expectation. Then the PDF of $\{\boldsymbol{r}_i\}_{i=1}^N$ conditioned on H_m is derived as

$$f_{\text{(Q)HLRT}}(\{\boldsymbol{r}_i\}_{i=1}^N|H_m) = \mathbb{E}_{\boldsymbol{s}^{(m)}}\left[f(\{\boldsymbol{r}_i\}_{i=1}^N, \{\hat{\boldsymbol{u}}_i^{(m)}\}_{i=1}^N|\boldsymbol{s}^{(m)}, H_m)\right], \tag{2.6}$$

where $\{\hat{\boldsymbol{u}}_i^{(m)}\}_{i=1}^N$ denote the vectors of the unknown parameter estimates conditioned on H_m. Under the HLRT approach, we use the MLE of the unknown parameter vectors to substitute into (2.6). Because the transmitted symbols, $\{s_k^{(m)}\}_{k=1}^K$, are unknown, one can find the joint MLE of the unknown parameters by solving $\partial f(\{\boldsymbol{r}_i\}_{i=1}^N|\boldsymbol{s}^{(m)}, \{\boldsymbol{u}_i\}_{i=1}^N, H_m)/\partial\boldsymbol{u}_i = 0$, for $i = 1, \cdots N$. After some manipulations, the MLE of the unknown channel coefficients and noise variances, given $\boldsymbol{s}^{(m)}$ is transmitted, can be expressed as,

$$\hat{h}_i^{(m)} = \frac{\boldsymbol{s}^{(m)H}\boldsymbol{r}_i}{\|\boldsymbol{s}^{(m)}\|^2}, \tag{2.7}$$

$$\widehat{\sigma_i^2}^{(m)} = \frac{1}{K}\left(\|\boldsymbol{r}_i\|^2 - \frac{|\boldsymbol{s}^{(m)H}\boldsymbol{r}_i|^2}{\|\boldsymbol{s}^{(m)}\|^2}\right), \tag{2.8}$$

where $\hat{h}_i^{(m)} = \hat{\alpha}_i^{(m)}e^{j\hat{\varphi}_i^{(m)}}$ for $i = 1, \cdots, N$. Substituting (2.7) and (2.8) into (2.6), taking $\log(\cdot)$, and after some algebraic simplifications, the LLF under HLRT is given by

$$\mathrm{LLF}_{\mathrm{HLRT}}(\{\boldsymbol{r}_i\}_{i=1}^N|H_m) = \log\left(\sum_{\zeta=1}^{M_m^K}\frac{1}{M_m^K}\prod_{i=1}^{N}[1-\rho_{i,\zeta}^{(m)2}]^{-K}\right), \tag{2.9}$$

where $\rho_{i,\zeta}^{(m)} = |\boldsymbol{s}_\zeta^{(m)H}\boldsymbol{r}_i|/(\|\boldsymbol{s}_\zeta^{(m)}\|\|\boldsymbol{r}_i\|)$ is the correlation coefficient between $\boldsymbol{s}_\zeta^{(m)}$ and $\boldsymbol{r}_i$. Here, $\boldsymbol{s}_\zeta^{(m)}$ indicates a sequence of K symbols each drawn independently from $\mathcal{S}_m$. Since the MLE employed under the HLRT algorithm are function of $\boldsymbol{s}^{(m)}$, we have to take into account all symbol sequences with the length K, which leads to the computational complexity of the order of $\mathcal{O}(NM_m^K)$ given H_m, which grows exponentially with the number of observation time slots, K. To resolve this complexity issue, one can use a non-MLE of the unknown parameters leading to the QHLRT algorithm [5, 6, 7], which is presented in the next subsection.

QHLRT

Under QHLRT, a non-MLE of the unknown parameters, which does not depend on the transmitted symbols, is used in (2.6) for blind MC. It has been shown that the QHLRT-based classifier yields similar classification performance to HLRT with substantially lower complexity [6]. There is no unique non-MLE for the unknown parameters. One common approach to find the parameter estimates is the method of moments (MoM) [5, 6, 7] and the corresponding algorithm is referred to as QHLRT-MoM. In [5, 6, 7], an algorithm which is based on the second- and fourth-order moments of the received signal has been used to estimate the unknown channel amplitude and noise variance, and the estimation method is referred to as $\mathrm{M_2M_4}$ in [18]. Denoting $\Upsilon^m = \mathbb{E}[|s^{(m)}|^4]/(\mathbb{E}[|s^{(m)}|^2])^2$, the $\mathrm{M_2M_4}$ estimates of channel amplitudes and noise variances, conditioned on H_m, are given by [6]

$$\hat{\alpha}_i^{(m)} = \Big(\frac{\hat{\mathcal{Z}}_{i,42} - 2\hat{\mathcal{Z}}_{i,21}^2}{\Upsilon^m - 2}\Big)^{1/4} (\mathbb{E}[|s^{(m)}|^2])^{-1/2}, \tag{2.10}$$

$$\widehat{\sigma_i^{2(m)}} = \hat{\mathcal{Z}}_{i,21} - \Big(\frac{\hat{\mathcal{Z}}_{i,42} - 2\hat{\mathcal{Z}}_{i,21}^2}{\Upsilon^m - 2}\Big)^{1/2}, \tag{2.11}$$

where $\hat{\mathcal{Z}}_{i,21}$ and $\hat{\mathcal{Z}}_{i,42}$ are the estimates of the second-order/ one conjugate and fourth-order/ two conjugate moments of the received signal, obtained by $\hat{\mathcal{Z}}_{i,21} = K^{-1}\sum_{k=1}^{K}|r_{i,k}|^2$ and $\hat{\mathcal{Z}}_{i,42} = K^{-1}\sum_{k=1}^{K}|r_{i,k}|^4$ respectively for $i = 1, \cdots N$. Note that Υ^m is determined by the modulation scheme, *i.e.*, the modulation corresponding to H_m. For instance, Υ^m is equal to 1 for M-PSK, and 1.32 for 16-QAM [15]. The phase estimates used in [5, 7], are expressed as in [14]

$$\hat{\varphi}_{\mathrm{PSK,i}}^{(m)} = M_m^{-1} \sphericalangle \Big(\sum_{k=1}^{K} r_{i,k}^{M_m}\Big), \tag{2.12}$$

$$\hat{\varphi}_{\mathrm{QAM,i}} = 4^{-1} \sphericalangle \Big(\sum_{k=1}^{K} r_{i,k}^{4}\Big). \tag{2.13}$$

Note that the estimates derived in (2.10)–(2.13) do not depend on $\boldsymbol{s}^{(m)}$. Hence, $\mathbb{E}_{\boldsymbol{s}^{(m)}}$ in (2.6) factors in K separate expectations and the computational complexity of QHLRT-MoM will be of the order of $\mathcal{O}(KM_m)$, which is much lower than HLRT. Substituting the QHLRT-MoM estimates (2.10) and (2.13) into (2.6), an MC scheme was proposed in[5] for multiple antennas with unknown channel amplitude and phase. Assuming unknown channel amplitude, phase, and noise variance, it is not difficult to extend the scheme proposed in [5]. The extended LLF given H_m is given by

$$\mathrm{LLF}_{\mathrm{MoM}}(\{\boldsymbol{r}_i\}_{i=1}^{N}|H_m) = \sum_{k=1}^{K} \log\Big(\sum_{p=1}^{M_m} \frac{1}{M_m} \prod_{i=1}^{N} \hat{\mathcal{R}}_{i,k,p}^{(m)}\Big), \tag{2.14}$$

where

$$\hat{\mathcal{R}}_{i,k,p}^{(m)} = \frac{1}{\widehat{\sigma_i^{2(m)}}} \exp\left(-\frac{\left|r_{i,k} - \hat{\alpha}_i^{(m)} e^{j\hat{\varphi}_i^{(m)}} s_{k,p}^{(m)}\right|^2}{\widehat{\sigma_i^{2(m)}}}\right).$$

The estimated modulation is obtained by replacing (2.14) with $f(\{\boldsymbol{r}_i\}_{i=1}^{N}|H_m)$ in (2.4).

2.3.2 Proposed Algorithm

The M_2M_4 estimates are the conventional ones which are not accurate enough for SIMO. Recently, an estimate was proposed in [18] based on the fourth-order moment of the received signal for a SIMO configuration which does not require a-priori knowledge of the modulation type and it outperforms the conventional MoM methods including M_2M_4. The method is referred to as the M_4 method and we employ it in our proposed QHLRT-based algorithm for SIMO. Assuming $\sigma_i^2 = \sigma^2$ and $N \geq 2$, the channel amplitudes and noise variance estimates of the M_4 method are obtained by

$$\widehat{\sigma^2}_{\mathrm{M}_4} = \frac{\max\left(0, \sum_{i=1}^{N}\sum_{l=i+1}^{N}(\hat{\mathcal{Z}}_{4,i,i}^{1/2} + \hat{\mathcal{Z}}_{4,l,l}^{1/2} - ((\hat{\mathcal{Z}}_{4,i,i}^{1/2} - \hat{\mathcal{Z}}_{4,l,l}^{1/2})^2 + 4\hat{\mathcal{Z}}_{4,i,l}^{1/2})^{1/2})\right)}{N(N-1)}, \quad (2.15)$$

$$\hat{\alpha}_{i,\mathrm{M}_4} = \max\left(0, (\hat{\mathcal{Z}}_{4,i,i} - \widehat{\sigma^2}_{\mathrm{M}_4})^{1/2}\right), \quad (2.16)$$

where $\hat{\mathcal{Z}}_{4,i,l} = \max(0, \sum_{k=1}^{K} \Re\{r_{i,k+1}r_{i,k}^{*}r_{l,k+1}^{*}r_{l,k}\})/(K-1)$. We refer interested readers to [18] for more details of estimates for nonuniform noise variances. In this work, M_4 method is employed to perform MC for the first time.

The NDA channel phase estimates depend on the type of the hypothesized modulation scheme. We denote $\tilde{\varphi}_i = 1/2 \arctan(2(\hat{\mathcal{Z}}_{\Re,\Im,i} - \hat{\mathcal{Z}}_{\Re,i}\hat{\mathcal{Z}}_{\Im,i})/(\hat{\mathcal{Z}}_{\Re,2,i} - \hat{\mathcal{Z}}_{\Re,i}^2 - \hat{\mathcal{Z}}_{\Im,2,i} + \hat{\mathcal{Z}}_{\Im,i}^2))$ where $\hat{\mathcal{Z}}_{\Re,i}$, $\hat{\mathcal{Z}}_{\Im,i}$, $\hat{\mathcal{Z}}_{\Re,2,i}$, $\hat{\mathcal{Z}}_{\Im,2,i}$, and $\hat{\mathcal{Z}}_{\Re,\Im,i}$ are the sample averages, *i.e.*, $\sum_{k=1}^{K}(\cdot)/K$ of $r_{\Re,i,k}$, $r_{\Im,i,k}$, $r_{\Re,i,k}^2$, $r_{\Im,i,k}^2$, and $r_{\Re,i,k}r_{\Im,i,k}$, respectively. Here, $r_{\Re,i,k}$ and $r_{\Im,i,k}$ indicate the real and imaginary parts of $r_{i,k}^4$. Using the NDA phase estimates proposed in [17] for QAM, we have

$$\hat{\varphi}_{\mathrm{QAM},i} = \begin{cases} \tilde{\varphi}_i/4 & \text{if} \quad -\pi/2 + \tilde{\varphi}_i \le \psi_i \le \pi/2 + \tilde{\varphi}_i \ (0 \le \tilde{\varphi}_i \le \pi/2), \\ (\tilde{\varphi}_i - \pi)/4 & \text{otherwise} \quad (0 \le \tilde{\varphi}_i \le \pi/2), \\ \tilde{\varphi}_i/4 & \text{if} \quad -\pi/2 + \tilde{\varphi}_i \le \psi_i \le \pi/2 + \tilde{\varphi}_i \ (-\pi/2 \le \tilde{\varphi}_i \le 0), \\ (\tilde{\varphi}_i + \pi)/4 & \text{otherwise} \quad (-\pi/2 \le \tilde{\varphi}_i \le 0), \end{cases} \tag{2.17}$$

where $\psi_i = \arctan(\hat{\mathcal{Z}}_{\Im,i}/\hat{\mathcal{Z}}_{\Re,i})$. To estimate phase for PSK signals, (2.12) is used.

Denoting LLF_i as the LLF of the received signal from the i-th branch and using (2.15)–(2.17), we have

$$\mathrm{LLF}_i(\boldsymbol{r}_i|H_m) = \sum_{k=1}^{K} \log\left(\frac{1}{M_m}\sum_{p=1}^{M_m}\frac{1}{\widehat{\sigma^2}_{\mathrm{M}_4}}\exp\left(-\frac{\left|r_{i,k} - \hat{\alpha}_{i,\mathrm{M}_4}e^{j\hat{\varphi}_i^{(m)}}s_{k,p}^{(m)}\right|^2}{\widehat{\sigma^2}_{\mathrm{M}_4}}\right)\right), \tag{2.18}$$

for $i = 1, \cdots, N$. Using the WS scheme, we take a linear combination of the LLFs of N receiving antennas to perform blind MC. In order to address the problem of QHLRT-MoM, we propose that the LLF corresponding to the m-th hypothesis is expressed as

$$\mathrm{LLF}_{\mathrm{WS}}(\{\boldsymbol{r}_i\}_{i=1}^N|H_m) = \sum_{i=1}^{N}\lambda_i \mathrm{LLF}_i(\boldsymbol{r}_i|H_m), \tag{2.19}$$

where $\{\lambda_i\}_{i=1}^N$ are constants such that $\sum_{i=1}^N \lambda_i = 1$. One can note that based on the structure of (2.19), small values due to inaccurate estimates do not affect the entire expression, *i.e.,* $\sum_{i=1}^N \lambda_i \mathrm{LLF}_i$ will not approach zero if $\min\{\mathrm{LLF}_i\} \approx 0$. Hence, the problem of (2.14) is resolved.

One possibility to determine $\{\lambda_i\}_{i=1}^N$ is to maximize the average probability of correct classification, *i.e.,*

$$(\lambda_{1,\mathrm{opt}}, \cdots, \lambda_{N,\mathrm{opt}}) = \arg\max_{(\lambda_1,\cdots,\lambda_N)} \mathrm{Pr}_{CC}(\lambda_1, \cdots, \lambda_N), \tag{2.20}$$

where

$$\Pr_{CC} = N_{\text{mod}}^{-1} \sum_{m=1}^{N_{\text{mod}}} \Pr(\text{correct}|H_m), \tag{2.21}$$

and $\Pr(\text{correct}|H_m)$ denotes the conditional probability of correct classification given m-th modulation is actually transmitted. In the literature, the approximate analytical expression of $\Pr_{CC}$ is proposed only for the case of SISO configuration with no-unknown parameters, *i.e.,* ALRT-UB [16]. Unfortunately, it is difficult to derive an analytical expression of $\Pr_{CC}$ of QHLRT even for SISO.

Using the Cauchy-Schwarz inequality, we have

$$\sum_{i=1}^{N} \lambda_i \text{LLF}_i(\boldsymbol{r}_i|H_m) \leq \sqrt{\Big(\sum_{i=1}^{N} \lambda_i^2\Big)\Big(\sum_{i=1}^{N} \text{LLF}_i^2(\boldsymbol{r}_i|H_m)\Big)}, \tag{2.22}$$

with the equality holds if and only if $\lambda_i = \zeta \text{LLF}_i(\boldsymbol{r}_i|H_m)$ for $i = 1, \cdots, N$ and some constant ζ. The constant ζ is given by substituting $\{\lambda_i\}_{i=1}^{N}$ into $\sum_{i=1}^{N} \lambda_i = 1$. The coefficient $\lambda_{i,\text{WS}}$ which is substituted to (2.19) is obtained by

$$\lambda_{i,\text{WS}} = \frac{\text{LLF}_i(\boldsymbol{r}_i|H_m)}{\sum_{i=1}^{N} \text{LLF}_i(\boldsymbol{r}_i|H_m)} \tag{2.23}$$

for $i = 1, \cdots, N$. One can note that if $\text{LLF}_i(\boldsymbol{r}_i|H_m) \geq \text{LLF}_j(\boldsymbol{r}_j|H_m)$, then $\lambda_{i,\text{WS}} \geq \lambda_{j,\text{WS}}$, *i.e.,* the LF of the i-th antenna contributes more to the final decision. Asymptotically, if one of the LFs is substantially greater than all other LFs, the corresponding coefficient will approach one which is an appealing property of (2.23). The performance improvement of the proposed scheme will be demonstrated in Section 2.5.

2.4 Performance Upper Bounds and CRLB Analysis

2.4.1 ALRT-UB

If perfect knowledge of the CSI and noise variances of all branches, $\{\boldsymbol{u}_i\}_{i=1}^{N}$, were available at the receiver side, there would be no need to perform $\mathbb{E}_{\{\boldsymbol{u}_i\}_{i=1}^{N}}[\cdot]$. This approach, which is referred to as ALRT-UB [7], provides an upper bound on the performance of any MC algorithm. One can straightforwardly show that the LF under the m-th hypothesis is given by

$$f_{\text{ALRT-UB}}(\{\boldsymbol{r}_i\}_{i=1}^{N}|H_m) = \prod_{k=1}^{K} \frac{1}{M_m} \sum_{p=1}^{M_m} \prod_{i=1}^{N} (\pi\sigma_i^2)^{-1} \exp\left(-\frac{|r_{i,k} - \alpha_i e^{j\varphi_i} s_{k,p}^{(m)}|^2}{\sigma_i^2}\right). \tag{2.24}$$

2.4.2 QHLRT-UB

In order to evaluate the accuracy of QHLRT-MoM estimates, one needs an upper bound on the performance of QHLRT-based classifiers as a benchmark. For unbiased joint estimates of the unknown parameters, using the CRLBs as the variances of the estimates provides an upper bound on the classification performance [7]. For the sake of comparison, we assume optimum estimates which achieve the CRLBs. In QHLRT upper bound (QHLRT-UB), we assume the parameter estimates that are normally distributed. The LF under the $m-$th hypothesis is expressed as

$$f_{\text{QHLRT-UB}}(\{\boldsymbol{r}_i\}_{i=1}^{N}|H_m) = \prod_{k=1}^{K} \frac{1}{M_m} \sum_{p=1}^{M_m} \prod_{i=1}^{N} (\pi\widetilde{\sigma_i^{2(m)}})^{-1} \exp\left(-\frac{|r_{i,k} - \tilde{\alpha}_i^{(m)} e^{j\tilde{\varphi}_i^{(m)}} s_{k,p}^{(m)}|^2}{\widetilde{\sigma_i^{2(m)}}}\right), \tag{2.25}$$

where $\tilde{\alpha}_i^{(m)} \sim \mathcal{N}\big(\alpha_i, \mathrm{CRLB}(\hat{\alpha}_i^{(m)})\big)$, $\tilde{\varphi}_i^{(m)} \sim \mathcal{N}\big(\varphi_i, \mathrm{CRLB}(\hat{\varphi}_i^{(m)})\big)$, and $\widetilde{\sigma_i^{2(m)}} \sim \mathcal{N}\big(\sigma_i^2, \mathrm{CRLB}(\widehat{\sigma_i^{2(m)}})\big)$.

2.4.3 CRLBs of QHLRT-UB

The true joint CRLBs for SIMO configuration are obtained by considering $[\boldsymbol{u}_1^\dagger, \boldsymbol{u}_2^\dagger, \cdots, \boldsymbol{u}_N^\dagger]^\dagger$ as the unknown parameter vector. Since taking expectation with respect to the LF (2.24) is analytically intractable, we resort to the exact CRLBs for SISO configuration. In [19] and [20], the CRLBs of square QAM are derived for unknown SNR and phase respectively. Those results cannot be directly extended to the general rectangular QAM because the corresponding LLFs are different. To the best of our knowledge, the CRLBs for rectangular $I \times J$-QAM with amplitude, phase, and noise variance as the unknown parameters have not been derived in the literature. In this thesis, we tackle this problem.

For notational simplicity, we drop the subscript i and superscript (m) in the following equations. The QHLRT-UB estimates are obtained by $\hat{\alpha} \sim \mathcal{N}\big(\alpha, \mathrm{CRLB}(\hat{\alpha})\big)$, $\hat{\varphi} \sim \mathcal{N}\big(\varphi, \mathrm{CRLB}(\hat{\varphi})\big)$, and $\widehat{\sigma^2} \sim \mathcal{N}\big(\sigma^2, \mathrm{CRLB}(\widehat{\sigma^2})\big)$. We first derive a simplified and closed-form expression for the LLF given that the received signal has rectangular $I \times J$-QAM modulation scheme and then using the simplified LLF, we obtain the CRLBs.

We take $2d_{I,J}$ to be the minimum distance between two adjacent constellation points of the rectangular $I \times J$-QAM constellation for $I = 2q$ and $J = 2t$ where q and t are arbitrary integers. Then the constellation points can be written as $\mathcal{S} = \{\pm(2l-1)d_{I,J} \pm j(2p-1)d_{I,J}\}$, for $l = 1, 2, \cdots, I/2$, $p = 1, 2, \cdots, J/2$. In order to have a unit variance rectangular $I \times J$-QAM constellation, we assume $d_{I,J} = \sqrt{\frac{3}{I^2+J^2-2}}$.

We use the notation $\gamma := \alpha^2/\sigma^2$ to represent the received SNR. Denoting $\{s_{k,p}\}_{p=1}^{IJ}$ as the possible transmitted symbols drawn from the constellation in the $k \in [1, K]$-th time slot and averaging over all constellation points, the conditional LF given the unknown parameter vector is obtained by

$$f(\boldsymbol{r}|\boldsymbol{u}) = \prod_{k=1}^{K} \frac{1}{\pi IJ\sigma^2} \sum_{p=1}^{IJ} \exp\left(-\frac{|r_k - \alpha e^{j\varphi} s_{k,p}|^2}{\sigma^2}\right). \tag{2.26}$$

The computational complexity of (2.26) is of the order of $\mathcal{O}(KIJ)$.

Lemma 2.1. *The conditional LLF in* (2.26) *can be simplified to*

$$LLF(\boldsymbol{r}|\boldsymbol{u}) = \mathcal{C} + \sum_{k=1}^{K}\left(\log\left(\sum_{l=1}^{I/2} g_l \cosh(u_l \Re\{r_k e^{-j\varphi}\})\right) + \log\left(\sum_{p=1}^{J/2} g_p \cosh(u_p \Im\{r_k e^{-j\varphi}\})\right)\right), \tag{2.27}$$

where $g_l = \exp\left(-\alpha^2 d_{I,J}^2[(2l-1)^2 - 1]/\sigma^2\right)$, $u_l = 2\alpha(2l-1)d_{I,J}/\sigma^2$ *for* $l = 1, 2, \cdots, I/2$, *and* $\mathcal{C} = K\log(\frac{4}{\pi IJ\sigma^2}) - 2K\alpha^2 d_{I,J}^2/\sigma^2 - \|\boldsymbol{r}\|^2/\sigma^2$.

Proof. Expanding the exponent term in (2.26) as $\exp\left(-\frac{|r_k|^2+\alpha^2|s_{k,p}|^2}{\sigma^2}\right)\exp\left(\frac{2\Re\{r_k \alpha e^{-j\varphi} s_{k,p}^*\}}{\sigma^2}\right)$ and combining four exponential terms corresponding to each pair of (l, p), *i.e.*, $\pm(2l-1)d_{I,J} \pm j(2p-1)d_{I,J}$, we have $f(\boldsymbol{r}|\boldsymbol{u}) = \prod_{k=1}^{K} 1/(\pi IJ\sigma^2)\exp\left(-|r_k|^2/\sigma^2\right)\sum_{l=1}^{I/2}\sum_{p=1}^{J/2}\xi_{l,p}$, where

$$\xi_{l,p} = 4\cosh(u_l \Re\{r_k e^{-j\varphi}\})\cosh(u_p \Im\{r_k e^{-j\varphi}\})\exp\left(-\frac{\alpha^2 d_{I,J}^2[(2l-1)^2 + (2p-1)^2]}{\sigma^2}\right). \tag{2.28}$$

After some algebraic simplifications, we obtain

$$f(\boldsymbol{r}|\boldsymbol{u}) = \prod_{k=1}^{K} \frac{4}{\pi IJ\sigma^2}\exp\left(-\frac{|r_k|^2 + 2\alpha^2 d_{I,J}^2}{\sigma^2}\right)\sum_{l=1}^{I/2} g_l \cosh(u_l \Re\{r_k e^{-j\varphi}\})\sum_{p=1}^{J/2} g_p \cosh(u_p \Im\{r_k e^{-j\varphi}\}). \tag{2.29}$$

Taking $\log(\cdot)$ to (2.29), (2.27) is obtained. □

Note that the complexity to compute $\mathrm{LLF}(\boldsymbol{r}|\boldsymbol{u})$ in (2.27) reduces to the order of $\mathcal{O}(K(I+J))$.

In order to find the CRLBs of the unknown parameters, one should derive the Fisher information matrix (FIM), which is denoted by $\mathcal{I}(\boldsymbol{u}) := [\mathcal{I}_{b,c}]$, for $b, c =$1, 2, and 3,

$$\mathcal{I}_{b,c} = -\mathbb{E}\left[\frac{\partial^2}{\partial u_b \partial u_c}\mathrm{LLF}(\boldsymbol{r}|\boldsymbol{u})\right], \tag{2.30}$$

where u_b is the b-th unknown parameter and $\mathrm{LLF}(\boldsymbol{r}|\boldsymbol{u})$ denotes the LLF of the received signal conditioned on the parameter vector.

Lemma 2.2. *The FIM for the unknown parameter vector assuming rectangular $I \times J$-QAM signal is given by*

$$\mathcal{I}(\boldsymbol{u}) = \frac{2K}{\sigma^4}\begin{pmatrix} \sigma^2 - \sigma^2\mathcal{G}_{I,J}(\gamma) & 0 & \alpha\mathcal{H}_{I,J}(\gamma) \\ 0 & \alpha^2\sigma^2\big(1-\mathcal{F}_{I,J}(\gamma)\big) & 0 \\ \alpha\mathcal{H}_{I,J}(\gamma) & 0 & \frac{1}{2} - \frac{\alpha^2}{\sigma^2}\mathcal{K}_{I,J}(\gamma) \end{pmatrix}, \tag{2.31}$$

where

$$\begin{cases} \mathcal{F}_{I,J}(\gamma) = (\frac{1}{2} + \gamma\frac{J^2-1}{I^2+J^2-2})\mathcal{F}_I(\gamma) + (\frac{1}{2} + \gamma\frac{I^2-1}{I^2+J^2-2})\mathcal{F}_J(\gamma), \\ \mathcal{G}_{I,J}(\gamma) = 1/2\big(\mathcal{G}_I(\gamma) + \mathcal{G}_J(\gamma)\big), \\ \mathcal{H}_{I,J}(\gamma) = 1/2\big(\mathcal{H}_I(\gamma) + \mathcal{H}_J(\gamma)\big), \\ \mathcal{K}_{I,J}(\gamma) = 1/2\big(\mathcal{K}_I(\gamma) + \mathcal{K}_J(\gamma)\big), \end{cases} \tag{2.32}$$

and $\mathcal{F}_I(\gamma)$, $\mathcal{G}_I(\gamma)$, $\mathcal{H}_I(\gamma)$ and $\mathcal{K}_I(\gamma)$ are given in the Appendix by (A.6), (A.12), (A.16), *and* (A.20) *respectively.*

Proof. See the Appendix. □

In the following theorems, we derive the CRLBs of the unknown parameters for rectangular $I \times J$-QAM and M-PAM, *i.e.*, for one- and two-dimensional amplitude modulation schemes.

Theorem 2.1. *The CRLBs of unbiased and joint estimates of α, φ, and σ^2 for rectangular $I \times J$-QAM with even I and J are given by*

$$CRLB_{I\times J\text{-}QAM}(\hat{\alpha}) = \frac{\alpha^2}{2K\gamma}\frac{1-2\gamma\mathcal{K}_{I,J}(\gamma)}{\mathcal{D}_{I,J}(\gamma)}, \tag{2.33}$$

$$CRLB_{I\times J\text{-}QAM}(\hat{\varphi}) = \frac{1}{2K\gamma}\frac{1}{1-\mathcal{F}_{I,J}(\gamma)}, \tag{2.34}$$

$$CRLB_{I\times J\text{-}QAM}(\widehat{\sigma^2}) = \frac{\sigma^4}{K}\frac{1-\mathcal{G}_{I,J}(\gamma)}{\mathcal{D}_{I,J}(\gamma)}, \tag{2.35}$$

where $\mathcal{D}_{I,J}(\gamma) = 1 - \mathcal{G}_{I,J}(\gamma) - 2\gamma\mathcal{K}_{I,J}(\gamma) + 2\gamma\left(\mathcal{G}_{I,J}(\gamma)\mathcal{K}_{I,J}(\gamma) - \mathcal{H}^2_{I,J}(\gamma)\right)$.

Proof. Taking the inverse of the FIM (2.31), (2.33)–(2.35) are obtained. □

The above theorem is applicable only for even I and J. In the following theorem, therefore, we provide the results for an M-PAM case.

Theorem 2.2. *The CRLBs, given the modulation scheme is M-PAM with even M, are given by*

$$CRLB_{M\text{-}PAM}(\hat{\alpha}) = \frac{\alpha^2}{2K\gamma}\frac{1-2\gamma\mathcal{K}_{M\text{-}PAM}(\gamma)}{\mathcal{D}_{M\text{-}PAM}(\gamma)}, \tag{2.36}$$

$$CRLB_{M\text{-}PAM}(\hat{\varphi}) = \frac{1}{2K\gamma}\frac{1}{1-\mathcal{F}_{M\text{-}PAM}(\gamma)}, \tag{2.37}$$

$$CRLB_{M\text{-}PAM}(\widehat{\sigma^2}) = \frac{\sigma^4}{K}\frac{1-\mathcal{G}_{M\text{-}PAM}(\gamma)}{\mathcal{D}_{M\text{-}PAM}(\gamma)}, \tag{2.38}$$

where $\mathcal{D}_{M\text{-}PAM}(\gamma) = 1 - \mathcal{G}_{M\text{-}PAM}(\gamma) - 2\gamma\mathcal{K}_{M\text{-}PAM}(\gamma) + 2\gamma\big(\mathcal{G}_{M\text{-}PAM}(\gamma)\mathcal{K}_{M\text{-}PAM}(\gamma) - \mathcal{H}^2_{M\text{-}PAM}(\gamma)\big)$ *and* $\mathcal{G}_{M\text{-}PAM}(\gamma)$, $\mathcal{F}_{M\text{-}PAM}(\gamma)$, $\mathcal{H}_{M\text{-}PAM}(\gamma)$, *and* $\mathcal{K}_{M\text{-}PAM}(\gamma)$ *are given by* (2.41).

Proof. Employing the approach used in Lemma 2.1, the conditional LLF given M-PAM signal is obtained by

$$\text{LLF}(\boldsymbol{r}|\boldsymbol{u}) = \mathcal{C}_{M\text{-PAM}} + \sum_{k=1}^{K}\log\left(\sum_{l=1}^{M/2} g_l\cosh(u_l\Re\{r_k e^{-j\varphi}\})\right), \tag{2.39}$$

where $\mathcal{C}_{M\text{-PAM}} = K\log(\frac{2}{\pi M\sigma^2}) - K\alpha^2 d^2/\sigma^2 - \|\boldsymbol{r}\|^2/\sigma^2$. To derive the FIM, one can follow the steps in the Appendix and obtain

$$\mathcal{I}_{M\text{-PAM}}(\boldsymbol{u}) = \frac{2K}{\sigma^4}\begin{pmatrix} \sigma^2 - \sigma^2\mathcal{G}_{M\text{-PAM}}(\gamma) & 0 & \alpha\mathcal{H}_{M\text{-PAM}}(\gamma) \\ 0 & \alpha^2\sigma^2\big(1-\mathcal{F}_{M\text{-PAM}}(\gamma)\big) & 0 \\ \alpha\mathcal{H}_{M\text{-PAM}}(\gamma) & 0 & \frac{1}{2} - \frac{\alpha^2}{\sigma^2}\mathcal{K}_{M\text{-PAM}}(\gamma) \end{pmatrix}, \tag{2.40}$$

where

$$\begin{cases} \mathcal{G}_{M\text{-PAM}}(\gamma) = \frac{2\exp(-\gamma d^2_{M\text{-PAM}})}{M\sqrt{2\pi}}\int_0^{+\infty}\frac{\exp(-x^2/2)\hat{\mathcal{G}}_{M\text{-PAM}}(x)}{\sum_{p=1}^{M/2} g_p\cosh(\sqrt{2\gamma}(2p-1)xd_{M\text{-PAM}})}\mathrm{d}x, \\ \mathcal{F}_{M\text{-PAM}}(\gamma) = \frac{2\exp(-\gamma d^2_{M\text{-PAM}})}{M\sqrt{2\pi}}\int_0^{+\infty}\frac{\exp(-x^2/2)\hat{\mathcal{F}}_{M\text{-PAM}}(x)}{\sum_{p=1}^{M/2} g_p\cosh(\sqrt{2\gamma}(2p-1)xd_{M\text{-PAM}})}\mathrm{d}x, \\ \mathcal{H}_{M\text{-PAM}}(\gamma) = \frac{2\exp(-\gamma d^2_{M\text{-PAM}})}{M\sqrt{2\pi}}\int_0^{+\infty}\frac{\exp(-x^2/2)\hat{\mathcal{H}}_{M\text{-PAM}}(x)}{\sum_{p=1}^{M/2} g_p\cosh(\sqrt{2\gamma}(2p-1)xd_{M\text{-PAM}})}\mathrm{d}x, \\ \mathcal{K}_{M\text{-PAM}}(\gamma) = \frac{2\exp(-\gamma d^2_{M\text{-PAM}})}{M\sqrt{2\pi}}\int_0^{+\infty}\frac{\exp(-x^2/2)\hat{\mathcal{K}}_{M\text{-PAM}}(x)}{\sum_{p=1}^{M/2} g_p\cosh(\sqrt{2\gamma}(2p-1)xd_{M\text{-PAM}})}\mathrm{d}x, \end{cases} \tag{2.41}$$

and $\hat{\mathcal{G}}_{M\text{-PAM}}(x)$, $\hat{\mathcal{F}}_{M\text{-PAM}}(x)$, $\hat{\mathcal{H}}_{M\text{-PAM}}(x)$, and $\hat{\mathcal{K}}_{M\text{-PAM}}(x)$ are obtained by substituting $I = M$ and $d_{M\text{-PAM}} = \sqrt{\frac{3}{M^2-1}}$ into the corresponding functions in (A.12), (A.6), (A.16), and (A.20) respectively. Taking the inverse of the FIM (2.40), (2.36)–(2.38) are derived which completes the proof. □

In the following, we provide the expressions of the CRLBs for special cases of Theorems 2.1 and 2.2.

Corollary 2.1. *The CRLBs for square M-QAM are simplified as follows:*

$$CRLB_{M\text{-}QAM}(\hat{\alpha}) = \frac{\alpha^2}{2K\gamma}\frac{1-2\gamma\mathcal{K}_{M\text{-}QAM}(\gamma)}{\mathcal{D}_{M\text{-}QAM}(\gamma)}, \tag{2.42}$$

$$CRLB_{M\text{-}QAM}(\hat{\varphi}) = \frac{1}{2K\gamma}\frac{1}{1-(1+\gamma)\mathcal{F}_{M\text{-}QAM}(\gamma)}, \tag{2.43}$$

$$CRLB_{M\text{-}QAM}(\widehat{\sigma^2}) = \frac{\sigma^4}{K}\frac{1-\mathcal{G}_{M\text{-}QAM}(\gamma)}{\mathcal{D}_{M\text{-}QAM}(\gamma)}, \tag{2.44}$$

where $\mathcal{D}_{M\text{-}QAM}(\gamma) = 1 - \mathcal{G}_{M\text{-}QAM}(\gamma) - 2\gamma\mathcal{K}_{M\text{-}QAM}(\gamma) + 2\gamma\big(\mathcal{G}_{M\text{-}QAM}(\gamma)\mathcal{K}_{M\text{-}QAM}(\gamma) - \mathcal{H}^2_{M\text{-}QAM}(\gamma)\big)$ *and* $\mathcal{G}_{M\text{-}QAM}(\gamma)$, $\mathcal{F}_{M\text{-}QAM}(\gamma)$, $\mathcal{H}_{M\text{-}QAM}(\gamma)$, *and* $\mathcal{K}_{M\text{-}QAM}(\gamma)$ *are obtained by* (2.46).

Proof. Denoting $d_{M\text{-QAM}} = \sqrt{\frac{3}{2(M-1)}}$ and substituting $I = J = \sqrt{M}/2$ into (A.6), (A.12), (A.16), and (A.20), the FIM for M-ary square QAM is given by

$$\mathcal{I}_{M\text{-QAM}}(\boldsymbol{u}) = \frac{2K}{\sigma^4}\begin{pmatrix} \sigma^2 - \sigma^2\mathcal{G}_{M\text{-QAM}}(\gamma) & 0 & \alpha\mathcal{H}_{M\text{-QAM}}(\gamma) \\ 0 & \alpha^2\sigma^2\big(1-(1+\gamma)\mathcal{F}_{M\text{-QAM}}(\gamma)\big) & 0 \\ \alpha\mathcal{H}_{M\text{-QAM}}(\gamma) & 0 & \frac{1}{2} - \frac{\alpha^2}{\sigma^2}\mathcal{K}_{M\text{-QAM}}(\gamma) \end{pmatrix}, \tag{2.45}$$

where

$$\begin{cases} \mathcal{G}_{M\text{-QAM}}(\gamma) = \frac{4\exp(-\gamma d^2_{M\text{-QAM}})}{\sqrt{2\pi M}}\int_0^{+\infty}\frac{\exp(-x^2/2)\hat{\mathcal{G}}_{M\text{-QAM}}(x)}{\sum_{p=1}^{\sqrt{M}/2} g_p\cosh(\sqrt{2\gamma}(2p-1)xd_{M\text{-QAM}})}\mathrm{d}x, \\ \mathcal{F}_{M\text{-QAM}}(\gamma) = \frac{2\exp(-\gamma d^2_{M\text{-QAM}})}{\sqrt{2\pi M}}\int_0^{+\infty}\frac{\exp(-x^2/2)\hat{\mathcal{F}}_{M\text{-QAM}}(x)}{\sum_{p=1}^{\sqrt{M}/2} g_p\cosh(\sqrt{2\gamma}(2p-1)xd_{M\text{-QAM}})}\mathrm{d}x, \\ \mathcal{H}_{M\text{-QAM}}(\gamma) = \frac{4\exp(-\gamma d^2_{M\text{-QAM}})}{\sqrt{2\pi M}}\int_0^{+\infty}\frac{\exp(-x^2/2)\hat{\mathcal{H}}_{M\text{-QAM}}(x)}{\sum_{p=1}^{\sqrt{M}/2} g_p\cosh(\sqrt{2\gamma}(2p-1)xd_{M\text{-QAM}})}\mathrm{d}x, \\ \mathcal{K}_{M\text{-QAM}}(\gamma) = \frac{4\exp(-\gamma d^2_{M\text{-QAM}})}{\sqrt{2\pi M}}\int_0^{+\infty}\frac{\exp(-x^2/2)\hat{\mathcal{K}}_{M\text{-QAM}}(x)}{\sum_{p=1}^{\sqrt{M}/2} g_p\cosh(\sqrt{2\gamma}(2p-1)xd_{M\text{-QAM}})}\mathrm{d}x. \end{cases} \tag{2.46}$$

Note that $\hat{\mathcal{G}}_{M\text{-QAM}}(x)$, $\hat{\mathcal{F}}_{M\text{-QAM}}(x)$, $\hat{\mathcal{H}}_{M\text{-QAM}}(x)$, and $\hat{\mathcal{K}}_{M\text{-QAM}}(x)$ are obtained by substituting $I = \sqrt{M}$ and $d_{M\text{-QAM}}$ into the corresponding functions in (A.12), (A.6), (A.16), and (A.20) respectively. Also, $\mathcal{G}_{M\text{-PAM}}(\gamma) = \mathcal{G}_{M^2\text{-QAM}}(2\gamma)$, $\mathcal{F}_{M\text{-PAM}}(\gamma) = \mathcal{F}_{M^2\text{-QAM}}(2\gamma)$, $\mathcal{H}_{M\text{-PAM}}(\gamma) = \mathcal{H}_{M^2\text{-QAM}}(2\gamma)$, and $\mathcal{K}_{M\text{-PAM}}(\gamma) = \mathcal{K}_{M^2\text{-QAM}}(2\gamma)$. Taking the inverse of the FIM (2.45), (2.42)–(2.44) are obtained and the proof is complete. □

The results of Corollary 2.1 are essentially the same as the results reported in [19, 20], although the mathematical expressions look different. In Section 2.5, we demonstrate that they provide the same results.

Example 2.1. *For example, given the signal with 16-QAM modulation scheme is transmitted, using* (2.46)*, and after some manipulations, we can show that*

$$\mathcal{F}_{16\text{-}QAM}(\gamma) = \frac{\exp(-0.1\gamma)}{2\sqrt{2\pi}} \int_0^{+\infty} \frac{\exp(-x^2/2)\hat{\mathcal{F}}_{16\text{-}QAM}(x)}{\cosh(\sqrt{0.2\gamma}x) + \exp(-0.8\gamma)\cosh(3\sqrt{0.2\gamma}x)} \mathrm{d}x, \tag{2.47}$$

where $\hat{\mathcal{F}}_{16\text{-}QAM}(x) = 0.4{+}3.6\exp(-1.6\gamma){+}4\exp(-0.8\gamma)\cosh(\sqrt{0.2\gamma}x)\cosh(3\sqrt{0.2\gamma}x) - 2.4\exp(-0.8\gamma)\sinh(\sqrt{0.2\gamma}x)\sinh(3\sqrt{0.2\gamma}x)$.

$$\mathcal{G}_{16\text{-}QAM}(\gamma) = \frac{\exp(-0.1\gamma)}{\sqrt{2\pi}} \int_0^{+\infty} \frac{\exp(-x^2/2)\hat{\mathcal{G}}_{16\text{-}QAM}(x)}{\cosh(\sqrt{0.2\gamma}x) + \exp(-0.8\gamma)\cosh(3\sqrt{0.2\gamma}x)} \mathrm{d}x, \tag{2.48}$$

where $\hat{\mathcal{G}}_{16\text{-}QAM}(x) = \big(0.2{+}1.8\exp(-1.6\gamma)\big)x^2{+}(2x^2{+}2.56\gamma)\exp(-0.8\gamma)\cosh(\sqrt{0.2\gamma}x) \cosh(3\sqrt{0.2\gamma}x){-}\sqrt{18.432\gamma}x\exp(-0.8\gamma)\cosh(\sqrt{0.2\gamma}x)\sinh(3\sqrt{0.2\gamma}x){+}\sqrt{2.048\gamma}x\exp(-0.8\gamma) \sinh(\sqrt{0.2\gamma}x)\cosh(3\sqrt{0.2\gamma}x) - 1.2x^2\exp(-0.8\gamma)\sinh(\sqrt{0.2\gamma}x)\sinh(3\sqrt{0.2\gamma}x)$.

Similarly, we obtain

$$\mathcal{H}_{16\text{-}QAM}(\gamma) = \frac{\exp(-0.1\gamma)}{\sqrt{2\pi}} \int_0^{+\infty} \frac{\exp(-x^2/2)\hat{\mathcal{H}}_{16\text{-}QAM}(x)}{\cosh(\sqrt{0.2\gamma}x) + \exp(-0.8\gamma)\cosh(3\sqrt{0.2\gamma}x)} \mathrm{d}x, \tag{2.49}$$

where $\hat{\mathcal{H}}_{16\text{-}QAM}(x) = \big(0.2{+}1.8\exp(-1.6\gamma)\big)x^2{+}(2x^2{+}1.28\gamma)\exp(-0.8\gamma)\cosh(\sqrt{0.2\gamma}x) \cosh(3\sqrt{0.2\gamma}x){-}\sqrt{10.368\gamma}x\exp(-0.8\gamma)\cosh(\sqrt{0.2\gamma}x)\sinh(3\sqrt{0.2\gamma}x){+}\sqrt{1.152\gamma}x\exp(-0.8\gamma) \sinh(\sqrt{0.2\gamma}x)\cosh(3\sqrt{0.2\gamma}x) - 1.2x^2\exp(-0.8\gamma)\sinh(\sqrt{0.2\gamma}x)\sinh(3\sqrt{0.2\gamma}x)$.

$$\mathcal{K}_{16\text{-}QAM}(\gamma) = \frac{\exp(-0.1\gamma)}{\sqrt{2\pi}} \int_0^{+\infty} \frac{\exp(-x^2/2)\hat{\mathcal{K}}_{16\text{-}QAM}(x)}{\cosh(\sqrt{0.2\gamma}x) + \exp(-0.8\gamma)\cosh(3\sqrt{0.2\gamma}x)} \mathrm{d}x, \tag{2.50}$$

where $\hat{\mathcal{K}}_{16\text{-}QAM}(x) = \big(0.2{+}1.8\exp(-1.6\gamma)\big)x^2{+}(2x^2{+}0.64\gamma)\exp(-0.8\gamma)\cosh(\sqrt{0.2\gamma}x) \cosh(3\sqrt{0.2\gamma}x){-}\sqrt{4.608\gamma}x\exp(-0.8\gamma)\cosh(\sqrt{0.2\gamma}x)\sinh(3\sqrt{0.2\gamma}x){+}\sqrt{0.512\gamma}x\exp(-0.8\gamma) \sinh(\sqrt{0.2\gamma}x)\cosh(3\sqrt{0.2\gamma}x) - 1.2x^2\exp(-0.8\gamma)\sinh(\sqrt{0.2\gamma}x)\sinh(3\sqrt{0.2\gamma}x)$. *Then the CRLBs for joint estimates of the unknown parameters are given by* (2.42)–(2.44).

Corollary 2.2. *The CRLBs of the unknown parameters for QPSK and BPSK modulations are given by*

$$CRLB_{QPSK}(\hat{\alpha}) = \frac{\alpha^2}{2K\gamma}\frac{1-2\gamma\mathcal{G}_{QPSK}(\gamma)}{1-(2\gamma+1)\mathcal{G}_{QPSK}(\gamma)}, \tag{2.51}$$

$$CRLB_{QPSK}(\hat{\phi}) = \frac{1}{2K\gamma}\frac{1}{1-(1+\gamma)\mathcal{F}_{QPSK}(\gamma)}, \tag{2.52}$$

$$CRLB_{QPSK}(\widehat{\sigma^2}) = \frac{\sigma^4}{K}\frac{1-\mathcal{G}_{QPSK}(\gamma)}{1-(2\gamma+1)\mathcal{G}_{QPSK}(\gamma)}, \tag{2.53}$$

$$CRLB_{BPSK}(\hat{\alpha}) = \frac{\alpha^2}{2K\gamma}\frac{1-2\gamma\mathcal{G}_{BPSK}(\gamma)}{1-(2\gamma+1)\mathcal{G}_{BPSK}(\gamma)}, \tag{2.54}$$

$$CRLB_{BPSK}(\hat{\phi}) = \frac{1}{2K\gamma}\frac{1}{1-\mathcal{F}_{BPSK}(\gamma)}, \tag{2.55}$$

$$CRLB_{BPSK}(\widehat{\sigma^2}) = \frac{\sigma^4}{K}\frac{1-\mathcal{G}_{BPSK}(\gamma)}{1-(2\gamma+1)\mathcal{G}_{BPSK}(\gamma)}, \tag{2.56}$$

where

$$\begin{cases} \mathcal{G}_{QPSK}(\gamma) = \frac{2\exp(-\gamma/2)}{\sqrt{2\pi}}\int_0^{+\infty}\frac{\exp(-x^2/2)x^2}{\cosh(\sqrt{\gamma}x)}\mathrm{d}x, \\ \mathcal{F}_{QPSK}(\gamma) = \frac{2\exp(-\gamma/2)}{\sqrt{2\pi}}\int_0^{+\infty}\frac{\exp(-x^2/2)}{\cosh(\sqrt{\gamma}x)}\mathrm{d}x, \end{cases} \tag{2.57}$$

and

$$\begin{cases} \mathcal{G}_{BPSK}(\gamma) = \frac{2\exp(-\gamma)}{\sqrt{2\pi}}\int_0^{+\infty}\frac{\exp(-x^2/2)x^2}{\cosh(\sqrt{2\gamma}x)}\mathrm{d}x, \\ \mathcal{F}_{BPSK}(\gamma) = \frac{2\exp(-\gamma)}{\sqrt{2\pi}}\int_0^{+\infty}\frac{\exp(-x^2/2)}{\cosh(\sqrt{2\gamma}x)}\mathrm{d}x. \end{cases} \tag{2.58}$$

Proof. Assuming that the transmitted signal has QPSK modulation scheme and using Corollary 2.1, we can show that $\mathcal{G}_{\text{QPSK}}(\gamma) = \mathcal{H}_{\text{QPSK}}(\gamma) = \mathcal{K}_{\text{QPSK}}(\gamma)$. Furthermore, the expression of $\mathcal{F}_{M\text{-QAM}}(\gamma)$ in (2.46) can be simplified to $\mathcal{F}_{\text{QPSK}}(\gamma)$. By substituting $\mathcal{G}_{\text{QPSK}}(\gamma)$ into (2.42) and (2.44), one can derive (2.51) and (2.53). Finally, (2.52) is obtained by replacing $\mathcal{F}(\cdot)$ in (2.43) with $\mathcal{F}_{\text{QPSK}}(\gamma)$. One can derive (2.54)–(2.56) for BPSK similarly. □

The expressions of the CRLBs are identical to those reported in [7] where the derivations for BPSK and QPSK modulation schemes are obtained.

Estimating the unknown SNR is of interest in digital communication systems for adaptive modulation and power control. In the following lemma, the expression of the CRLB of the SNR estimate is derived. Since the performance of SNR estimates is measured using the logarithmic dB scale, $\eta(\boldsymbol{u}_\gamma) = 10\log_{10}\frac{\alpha^2}{\sigma^2}$ is employed in the following as the parameter transformation, where $\boldsymbol{u}_\gamma := [\alpha\ \sigma^2]^\dagger$ denotes the partial unknown parameter vector corresponding to SNR estimation.

Lemma 2.3. *The CRLB of the SNR estimate for rectangular $I \times J$-QAM signal is expressed as*

$$CRLB_{SNR}(\hat{\gamma}) = \frac{100}{K\ln^2(10)\gamma}\frac{2+\gamma\big(1-\mathcal{G}_{I,J}(\gamma)-4\mathcal{K}_{I,J}(\gamma)+4\mathcal{H}_{I,J}(\gamma)\big)}{\mathcal{D}_{I,J}(\gamma)}. \tag{2.59}$$

Proof. The partial FIM for rectangular $I \times J$-QAM is given by

$$\mathcal{I}(\boldsymbol{u}_\gamma) = \frac{2K}{\sigma^4}\begin{pmatrix} \sigma^2 - \sigma^2\mathcal{G}_{I,J}(\gamma) & \alpha\mathcal{H}_{I,J}(\gamma) \\ \alpha\mathcal{H}_{I,J}(\gamma) & \frac{1}{2}-\frac{\alpha^2}{\sigma^2}\mathcal{K}_{I,J}(\gamma) \end{pmatrix}. \tag{2.60}$$

The CRLB for the unknown SNR estimate is obtain by [21],

$$\text{CRLB}(\hat{\gamma}) = \frac{\partial\eta(\boldsymbol{u}_\gamma)^\dagger}{\partial\boldsymbol{u}_\gamma}\mathcal{I}^{-1}(\boldsymbol{u}_\gamma)\frac{\partial\eta(\boldsymbol{u}_\gamma)}{\partial\boldsymbol{u}_\gamma}, \tag{2.61}$$

where $\frac{\partial\eta(\boldsymbol{u}_\gamma)}{\partial\boldsymbol{u}_\gamma} = [\frac{20}{\alpha\ln(10)}\ \frac{-10}{\sigma^2\ln(10)}]^\dagger$ denotes the derivative of the parameter transformation with respect to the partial parameter vector. Substituting the FIM (2.60) into (2.61) and after some algebraic manipulations, (2.59) is obtained. □

Finally, the asymptotic behaviors of the CRLBs obtained in Theorem 2.1 and Lemma 2.3 are derived in the following lemma.

Lemma 2.4. *When γ tends to infinity, the CRLBs of the unknown amplitude, phase,* *noise variance, and SNR estimates for rectangular $I \times J$-QAM are given by*

$$CRLB_{Asym}(\hat{\alpha}) = \frac{\alpha^2}{2K\gamma}, \tag{2.62}$$

$$CRLB_{Asym}(\hat{\varphi}) = \frac{1}{2K\gamma}, \tag{2.63}$$

$$CRLB_{Asym}(\widehat{\sigma^2}) = \frac{\sigma^4}{K}, \tag{2.64}$$

$$CRLB_{Asym}(\hat{\gamma}) = \frac{100}{K \ln^2(10)}. \tag{2.65}$$

Proof. One can note that $\mathcal{F}_{I,J}(\gamma)$, $\mathcal{G}_{I,J}(\gamma)$, $\mathcal{H}_{I,J}(\gamma)$, and $\mathcal{K}_{I,J}(\gamma)$ approach zero as γ tends to infinity. In fact, these functions are all multiples of $\exp(-\gamma d^2)$. Also, from equations (A.6), (A.12), (A.16), and (A.20), one can show that the integrands approach zero when γ increases as well. This is because in the numerators of the integrands, there is multiplication of $g_l g_p$ in which both g_l and g_p approach zero exponentially, while there is only g_p in the denominator. In both numerator and denominator, these terms asymptotically dominate the $\cosh(\cdot)$ and $\sinh(\cdot)$ terms which are functions of $\sqrt{\gamma}$. Hence, substituting $\mathcal{F}_{I,J}(\gamma) = \mathcal{G}_{I,J}(\gamma) = \mathcal{H}_{I,J}(\gamma) = \mathcal{K}_{I,J}(\gamma) = 0$ into (2.33), (2.34), (2.35), and (2.59), we derive (2.62)–(2.65). □

The assymptotic behaviors of the CRLBs of amplitude, phase, noise variance and SNR estimates are verified by numerical integrations in Section 2.5.

2.5 Numerical Results

Numerical results for the CRLBs of unbiased estimates of channel amplitude, phase, noise variance, and SNR are presented. We provide simulation results to evaluate the probability of correct classification for QHLRT-based algorithms introduced in

(2.14) and (2.19). We compare the classification performance of the proposed WS and QHLRT-MoM algorithms with ALRT-UB and QHLRT-UB.

We assume a block Rayleigh fading environment. We set $h_i \sim \mathcal{CN}(0,1)$ for $i = 1, \cdots, N$. Unless otherwise mentioned, K is set to 100. We set $\sigma_i^2 = \sigma^2$ for $i = 1, \cdots, N$ and use σ^2 to adjust the SNR values. The number of Monte Carlo trials to find the probability of correct classifications given H_m is set to 10^4. We use the average probability of correct classification, $\Pr_{CC}$, to compare the performance of MC algorithms. For the purpose of simulations, the QHLRT-UB estimates of the unknown parameters for SIMO configuration are computed by using the SISO derivations and substituting the corresponding parameter vectors, *i.e.,* $\boldsymbol{u}_i$ for $i = 1, \cdots, N$. In order to be consistent with (2.15) and (2.16), we take the average over the estimated noise variances of receiving antennas and consider only nonnegative estimated amplitudes. Substituting QHLRT-UB estimates into (2.24), modulation schemes are classified. To compare the performance of the proposed and QHLRT-MoM schemes fairly, we employ (2.15)–(2.17) for both of the schemes since these estimates are shown to outperform the conventional ones.

Using (2.33)–(2.35), (2.36)–(2.38), (2.42)–(2.44) and substituting $\alpha = 1$, Figs. 2.1, 2.2, and 2.3 show the numerical results of $K\text{CRLB}(\hat{\alpha})$, $K\text{CRLB}(\hat{\varphi})$, and $K\text{CRLB}(\widehat{\sigma^2})$ respectively for BPSK, 4-PAM, 8-QAM, QPSK, and 16-QAM. One can notice that all curves decrease with SNR increase. As expected, for low SNR values, the CRLBs corresponding to BPSK and 4-PAM tend to converge and the same behavior is observed for QPSK and 16-QAM. In addition, the gap between all curves tends to zero when SNR increases which is consistent with the asymptotic CRLBs in (2.62)–(2.64). Fig. 2.4 shows the CRLB of the SNR estimate for BPSK, 4-PAM, 8-QAM, QPSK, and 16-QAM substituting $K = 100$ into (2.59). The asymptotic CRLB of the SNR is consistent with (2.65). One can see that the results for QPSK and 16-QAM are identical to the results reported in [19] for square QAM.

Simulation results of the QHLRT-MoM and proposed WS algorithms for the classification of BPSK and QPSK are shown in Fig. 2.5 with $N = 2$ and 4 receiving antennas. Then their performance is compared to ALRT-UB and QHLRT-UB. As expected, the proposed scheme significantly outperforms the QHLRT-MoM, *i.e.,* employing both (2.15)–(2.17) and WS algorithm is needed to improve the performance. In addition, QHLRT-UB and ALRT-UB provide upper bounds on the classification performance of both the proposed and QHLRT-MoM schemes, with QHLRT-UB leading to a tighter bound. It can be seen that the average probabilities of correct classification of ALRT-UB, QHLRT-UB, and the proposed WS scheme approach one when SNR increases. Increasing the number of receiving antennas improves the classification performance of all schemes except the QHLRT-MoM. The reason for the odd performance of the QHLRT-MoM scheme is inaccurate NDA estimates, specifically the phase estimate, yielding very small LFs as explained in Section 2.3.

Fig. 2.6 presents the classification performance of the QHLRT-MoM and proposed WS algorithms compared to ALRT-UB and QHLRT-UB when recognizing BPSK, 4-PAM, and 16-QAM with $N = 2$ and 4 receiving antennas. The observations are consistent with those in Fig. 2.5. Although the QHLRT-MoM scheme experiences an error floor, the proposed scheme achieves the upper bounds as SNR increases.

The classification performance of the QHLRT-MoM and proposed WS algorithms compared to ALRT-UB and QHLRT-UB versus K with SNR $= 2$ dB when recognizing BPSK, 4-PAM, and 16-QAM is shown in Fig. 2.7. One can see that increasing K

improves $\Pr_{CC}$ and the proposed WS scheme outperforms the QHLRT-MoM scheme for all values of K.

Fig. 2.8 shows the simulation results of QHLRT-UB when recognizing QPSK, 8-QAM, and 16-QAM for $N = 2, 3, 4$ with $K = 10$ and 100. As expected, in low SNR region where the estimates are not accurate, increasing the number of receiving antennas does not lead to the performance improvement. This confirms the poor performance of the QHLRT-MoM scheme where the non-optimal, NDA estimates are used. Furthermore, it can be seen that increasing the number of observed samples yields significant performance improvement.

2.6 Conclusion

In this chapter, we have explored LB algorithms for linear digital modulation classification. We have considered an SIMO configuration with channel amplitude, phase, and noise variance as the unknown parameters. We have generalized the existing algorithms and proposed a new WS-based QHLRT scheme employing the state-of-the-art NDA parameter estimates. The CRLBs for general rectangular $I \times J$-QAM and M-PAM modulations have been derived and further used to develop QHLRT-UB which provided an upper bound on the classification performance of QHLRT-based algorithms. Numerical results showed the accuracy of the CRLB expressions and confirmed that our results generalize the existing expressions in the literature. It is demonstrated that the new proposed algorithm, which was not computationally demanding, outperformed the QHLRT-MoM algorithm significantly. The classification performance of the proposed algorithm was very close to the upper bounds. It is shown that we needed to employ both new estimates and WS-based algorithm for

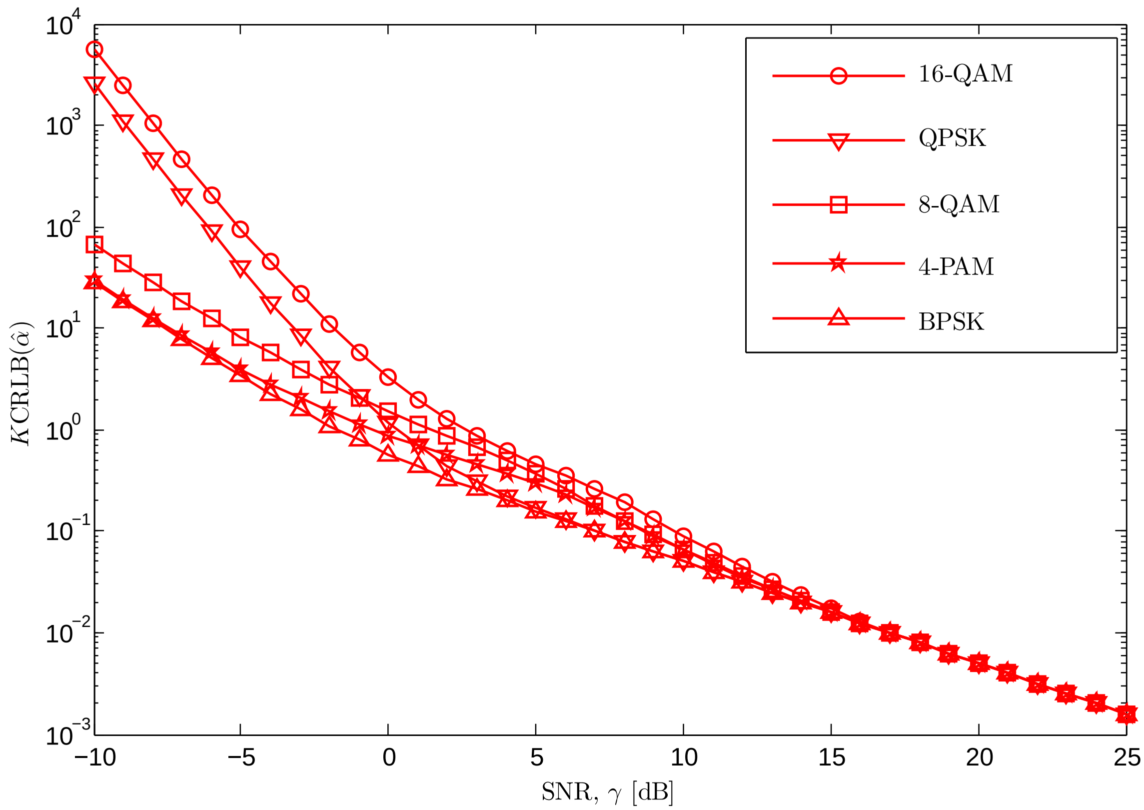

Figure 2.1: KCRLB($\hat{\alpha}$) versus SNR, γ, for BPSK, 4-PAM, 8-QAM, QPSK, and 16-QAM.

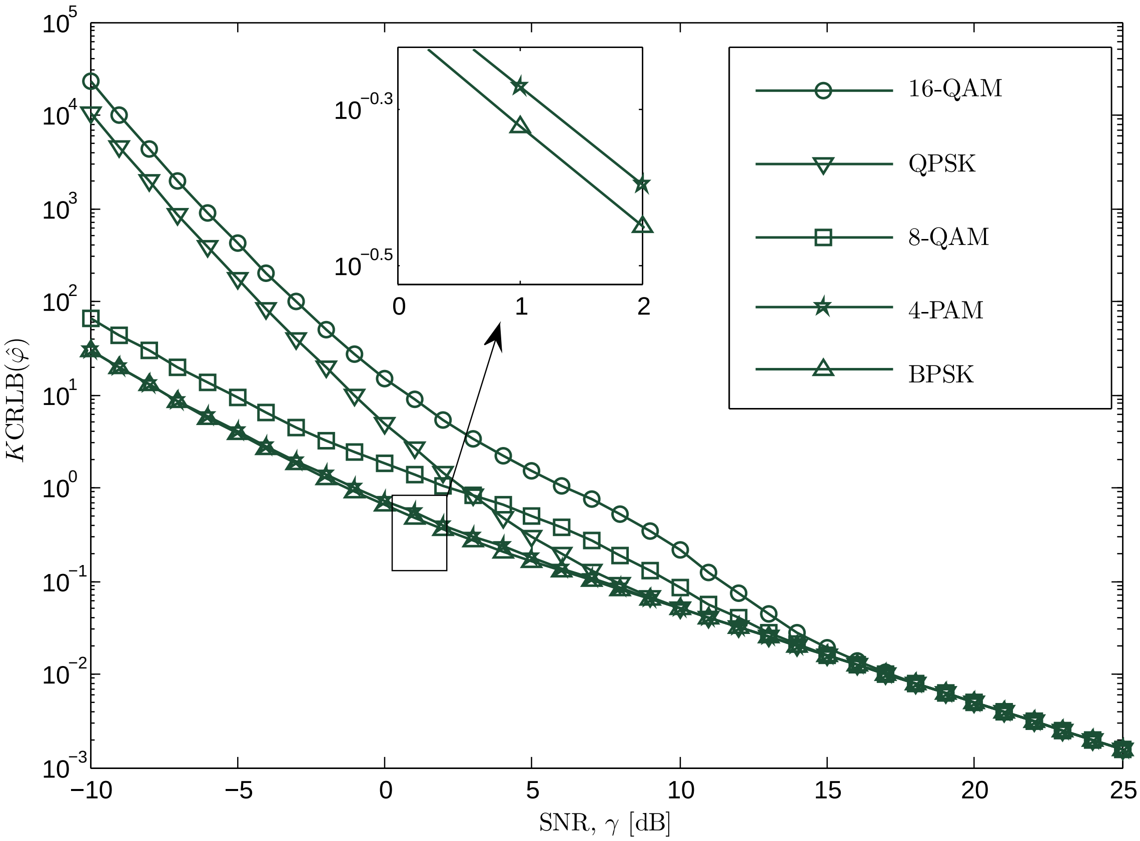

Figure 2.2: KCRLB($\hat{\varphi}$) versus SNR, γ, for BPSK, 4-PAM, 8-QAM, QPSK, and 16-QAM.

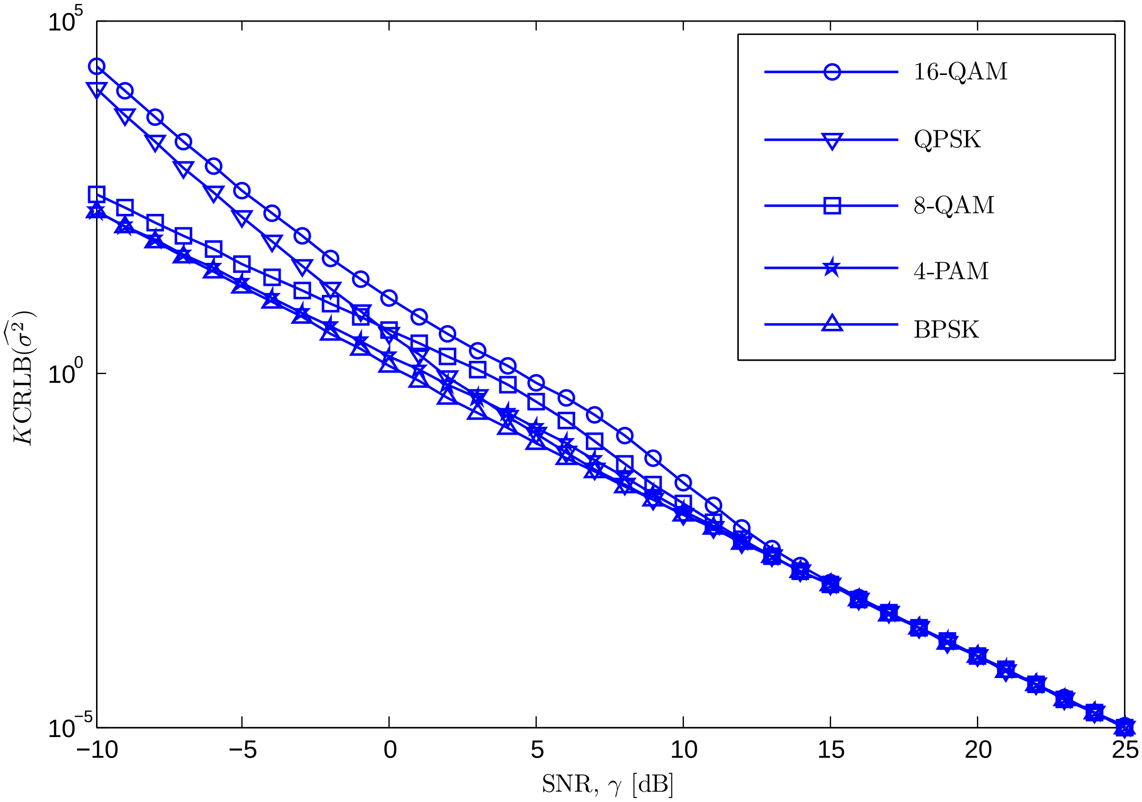

Figure 2.3: KCRLB$(\widehat{\sigma^2})$ versus SNR, γ, for BPSK, 4-PAM, 8-QAM, QPSK, and 16-QAM.

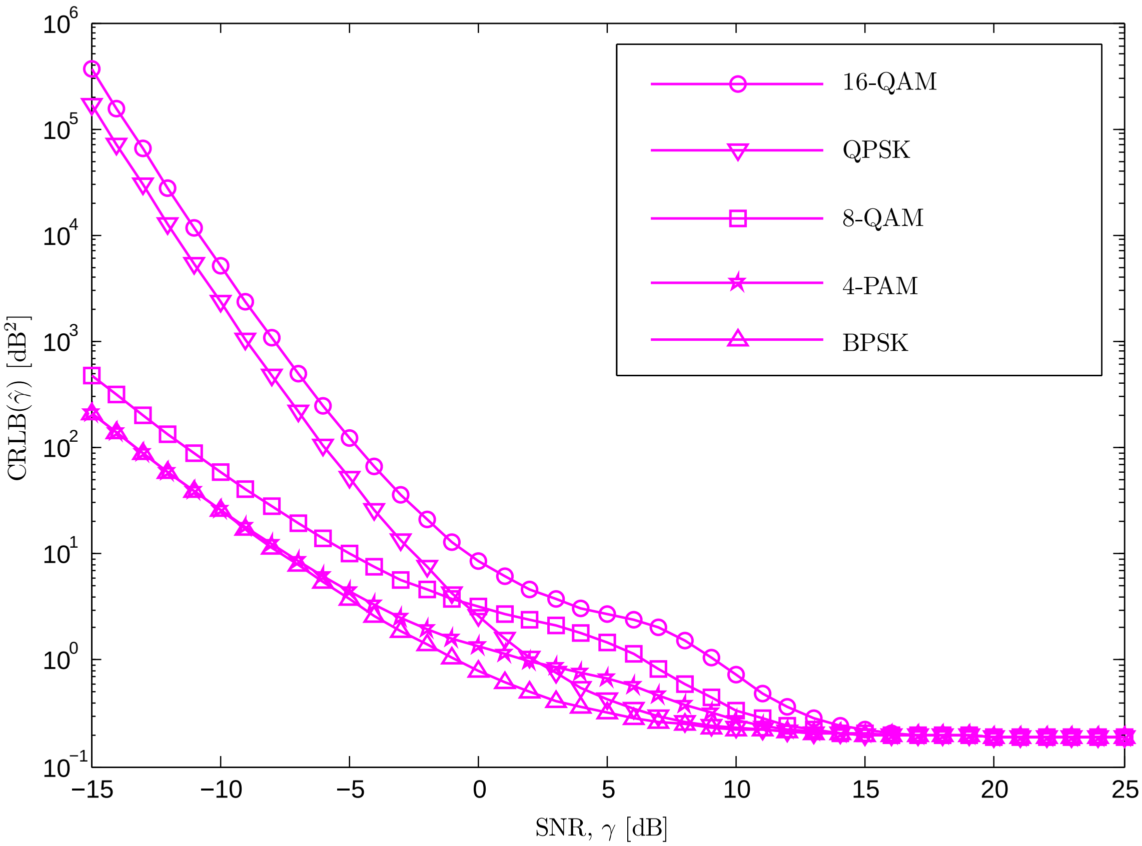

Figure 2.4: CRLB($\hat{\gamma}$) versus SNR, γ, for BPSK, 4-PAM, 8-QAM, QPSK, and 16-QAM for $K = 100$.

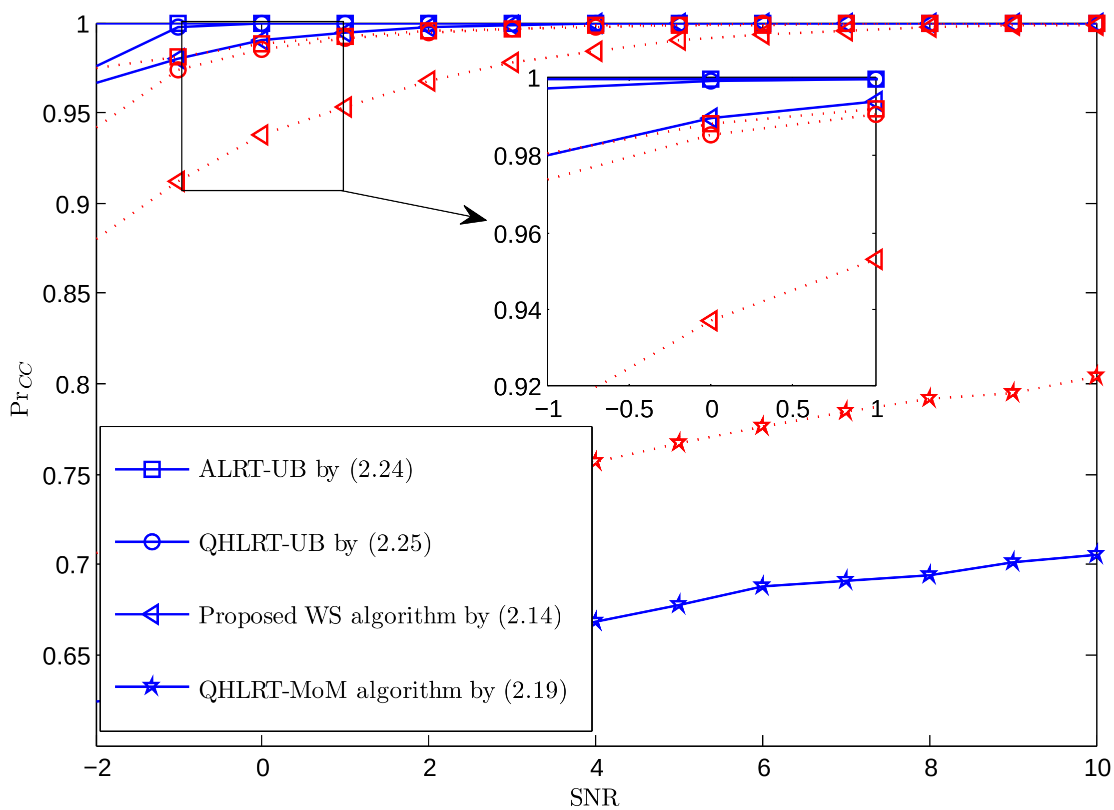

Figure 2.5: Performance of the QHLRT-MoM and proposed WS schemes compared to ALRT-UB and QHLRT-UB when recognizing BPSK and QPSK, with $K = 100$ for $N = 2$ (dashed lines) and $N = 4$ (solid lines).

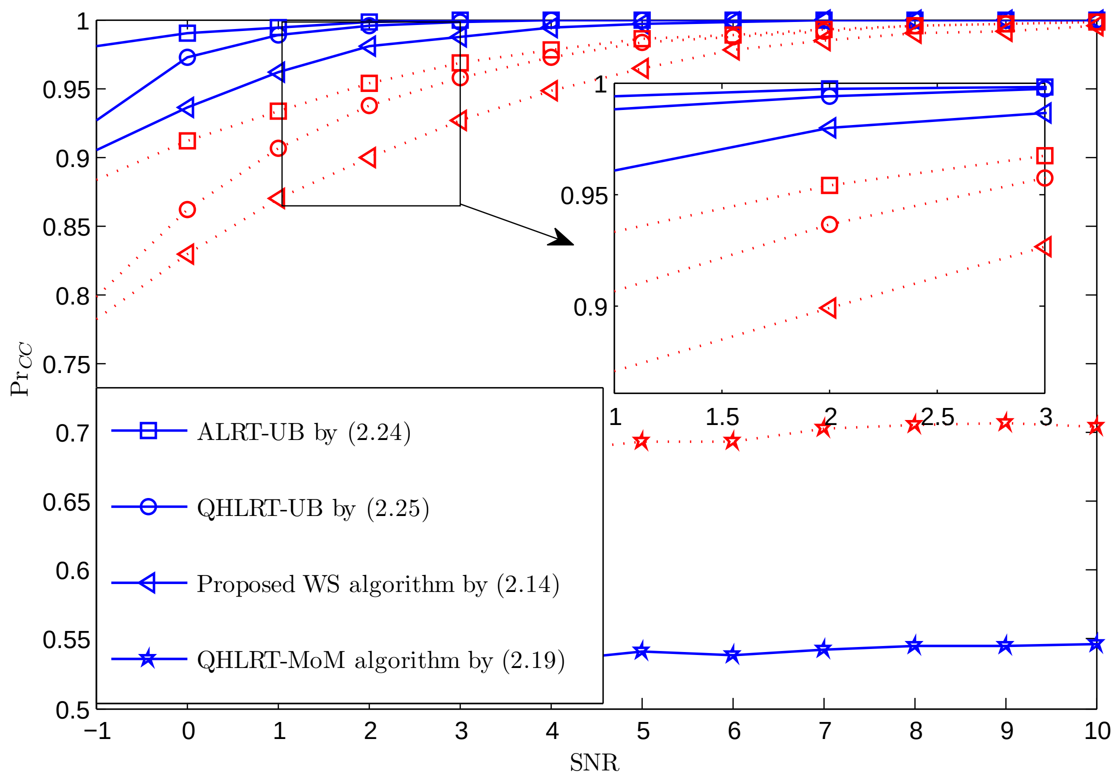

Figure 2.6: Performance of the QHLRT-MoM and proposed WS schemes compared to ALRT-UB and QHLRT-UB when recognizing BPSK, 4-PAM, and 16-QAM with $K = 100$ for $N = 2$ (dashed lines) and $N = 4$ (solid lines).

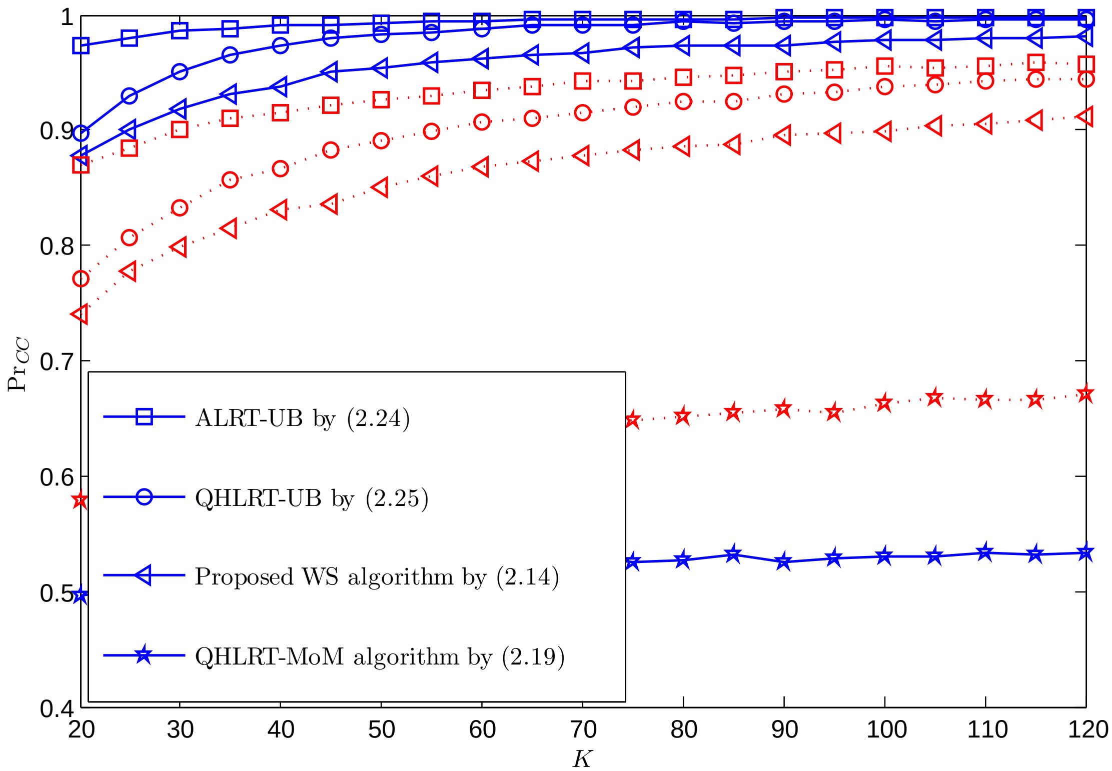

Figure 2.7: Performance of the QHLRT-MoM and proposed WS schemes compared to ALRT-UB and QHLRT-UB when recognizing BPSK, 4-PAM, and 16-QAM with SNR = 2 dB for $N = 2$ (dashed lines) and $N = 4$ (solid lines).

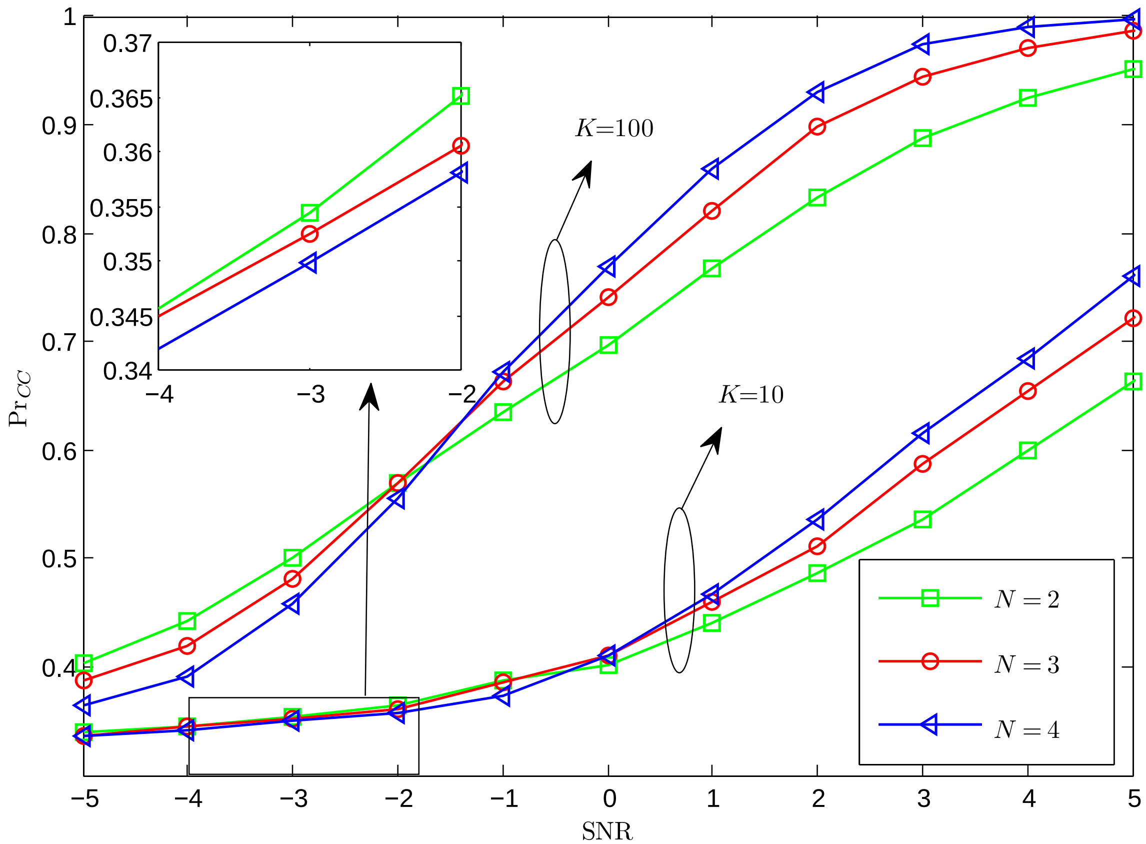

Figure 2.8: Performance of QHLRT-UB when recognizing QPSK, 8-QAM, and 16-QAM with $K = 10$ and $K = 100$ for $N = 2$, $N = 3$, and $N = 4$.

significant performance improvement.

2.7 Appendix: Proof of Lemma 2.2

Let us start with finding $\mathcal{I}_{2,2}$. Using (2.27) and denoting $\mathrm{LLF}_{I,k} := \log\Big(\sum_{l=1}^{I/2} g_l \cosh(u_l \Re\{r_k e^{-j\varphi}\})\Big)$, one can easily show that

$$\frac{\partial^2 \mathrm{LLF}_{I,k}}{\partial \varphi^2} = \frac{\sum_{p=1}^{I/2}\sum_{l=1}^{I/2} g_l g_p\Big(-\delta_{1,\varphi}(\Re\{r_k e^{-j\varphi}\}) + \Im^2\{r_k e^{-j\varphi}\}\big(\delta_{2,\varphi}(\Re\{r_k e^{-j\varphi}\}) - \delta_{3,\varphi}(\Re\{r_k e^{-j\varphi}\})\big)\Big)}{\big(\delta_I(\Re\{r_k e^{-j\varphi}\})\big)^2}, \tag{A.1}$$

where

$$\begin{cases} \delta_{1,\varphi}(\Re\{r_k e^{-j\varphi}\}) = u_l \Re\{r_k e^{-j\varphi}\} \sinh(u_l \Re\{r_k e^{-j\varphi}\}) \cosh(u_p \Re\{r_k e^{-j\varphi}\}), \\ \delta_{2,\varphi}(\Re\{r_k e^{-j\varphi}\}) = u_l^2 \cosh(u_l \Re\{r_k e^{-j\varphi}\}) \cosh(u_p \Re\{r_k e^{-j\varphi}\}), \\ \delta_{3,\varphi}(\Re\{r_k e^{-j\varphi}\}) = u_l u_p \sinh(u_l \Re\{r_k e^{-j\varphi}\}) \sinh(u_p \Re\{r_k e^{-j\varphi}\}), \\ \delta_I(\Re\{r_k e^{-j\varphi}\}) = \sum_{p=1}^{I/2} g_p \cosh(u_p \Re\{r_k e^{-j\varphi}\}). \end{cases} \tag{A.2}$$

Assuming $r_k = \alpha e^{j\varphi} s_{k,q} + n$, where n denotes AWGN, the real and imaginary parts of $r_k e^{-j\varphi}$ are given by $\alpha \Re\{s_{k,q}\} + v_{\Re}$ and $\alpha \Im\{s_{k,q}\} + v_{\Im}$ respectively, where $n e^{-j\varphi} = v_{\Re} + j v_{\Im}$. Denoting $\overline{\mathcal{F}}_I(\Re\{r_k e^{-j\varphi}\}) := -\sum_{p=1}^{I/2}\sum_{l=1}^{I/2} g_l g_p\, \delta_{1,\varphi}(\Re\{r_k e^{-j\varphi}\})$ and $\tilde{\mathcal{F}}_I(\Re\{r_k e^{-j\varphi}\}) := \sum_{p=1}^{I/2}\sum_{l=1}^{I/2} g_l g_p \Big(\delta_{2,\varphi}(\Re\{r_k e^{-j\varphi}\}) - \delta_{3,\varphi}(\Re\{r_k e^{-j\varphi}\})\Big)$, conditioned on that the known constellation point $s_{k,q}$ is transmitted, $\mathbb{E}[\mathrm{LLF}_{I,k}|s_{k,q}]$ is given by

$$\begin{aligned} &\frac{4\exp\Big(-\frac{2\alpha^2 d_{I,J}^2}{\sigma^2}\Big)}{\pi I J \sigma^2} \int_{-\infty}^{+\infty}\int_{-\infty}^{+\infty} \frac{\big(\overline{\mathcal{F}}_I(\alpha\Re\{s_{k,q}\}+v_{\Re}) + (\alpha\Im\{s_{k,q}\}+v_{\Im})^2 \tilde{\mathcal{F}}_I(\alpha\Re\{s_{k,q}\}+v_{\Re})\big)}{\delta_I(\alpha\Re\{s_{k,q}\}+v_{\Re})} \times \\ &\times \exp\Big(-\frac{(\alpha\Re\{s_{k,q}\}+v_{\Re})^2 + (\alpha\Im\{s_{k,q}\}+v_{\Im})^2}{\sigma^2}\Big)\, \delta_J(\alpha\Im\{s_{k,q}\} + v_{\Im}) \mathrm{d}v_{\Re} \mathrm{d}v_{\Im}. \end{aligned} \tag{A.3}$$

Changing the variables $\alpha\Re\{s_{k,q}\}+v_{\Re}=x$ and $\alpha\Im\{s_{k,q}\}+v_{\Im}=y$, we observe that $s_{k,q}$ vanishes from (A.3) and we have

$$\mathbb{E}\left[\frac{\partial^2 \mathrm{LLF}_{I,k}}{\partial\varphi^2}\right] = -\mathcal{J}_{1,I} + \frac{2\exp\left(-\frac{\alpha^2 d_{I,J}^2}{\sigma^2}\right)}{I\sqrt{\pi\sigma^2}}\mathcal{J}_{2,J}\int_{-\infty}^{+\infty}\frac{\exp(-\frac{x^2}{\sigma^2})\tilde{\mathcal{F}}_I(x)}{\delta_I(x)}\mathrm{d}x, \qquad \text{(A.4)}$$

where $\mathcal{J}_{1,I} = \frac{2\exp\left(-\frac{\alpha^2 d_{I,J}^2}{\sigma^2}\right)}{I\sqrt{\pi\sigma^2}}\int_{-\infty}^{+\infty}\exp(-\frac{x^2}{\sigma^2})x\sum_{l=1}^{I/2}u_l g_l\sinh(u_l x)\mathrm{d}x$ and $\mathcal{J}_{2,J} = \frac{2\exp\left(-\frac{\alpha^2 d_{I,J}^2}{\sigma^2}\right)}{J\sqrt{\pi\sigma^2}}$ $\int_{-\infty}^{+\infty}\exp(-\frac{y^2}{\sigma^2})\ y^2\delta_J(y)\mathrm{d}y$. Substituting $\{g_p,u_p\}_{p=1}^{J/2}$ into $\delta_J(y)$, we derive

$$\begin{aligned}\mathcal{J}_{2,J} &= \frac{1}{J\sqrt{\pi\sigma^2}}\int_{-\infty}^{+\infty}y^2\Big(\sum_{p=1}^{J/2}\exp\big(-\frac{(y-(2p-1)\alpha d_{I,J})^2}{\sigma^2}\big)+\exp\big(-\frac{(y+(2p-1)\alpha d_{I,J})^2}{\sigma^2}\big)\Big)\mathrm{d}y\\ &= \frac{2}{J}\Big(\sum_{p=1}^{J/2}\big(\sigma^2/2+\alpha^2 d_{I,J}^2(2p-1)^2\big)\Big). \qquad \text{(A.5)}\end{aligned}$$

Using $\sum_{p=1}^{J/2}(2p-1)^2 = J(J^2-1)/6$, we obtain $\mathcal{J}_{2,J} = \frac{\sigma^2}{2}+\alpha^2\frac{J^2-1}{I^2+J^2-2}$. Similarly, it is not difficult to show $\mathcal{J}_{1,I} = \frac{2\alpha^2}{\sigma^2}\frac{I^2-1}{I^2+J^2-2}$. Since $\{r_k\}_{k=1}^{K}$ are independent random variables, we have $\mathbb{E}[\frac{\partial^2\mathrm{LLF}_I(\boldsymbol{r}|\boldsymbol{u})}{\partial\varphi^2}] = K\mathbb{E}[\frac{\partial^2\mathrm{LLF}_{I,k}}{\partial\varphi^2}]$. Also, it is easy to show that $\mathbb{E}[\frac{\partial^2\mathcal{C}}{\partial\varphi^2}] = 0$. Substituting $\mathcal{J}_{1,I}$ and $\mathcal{J}_{2,J}$ into (A.4) and after some manipulations, we obtain $\mathcal{I}_{2,2} = 2K\gamma[1-(\frac{1}{2}+\gamma\frac{J^2-1}{I^2+J^2-2})\mathcal{F}_I(\gamma)-(\frac{1}{2}+\gamma\frac{I^2-1}{I^2+J^2-2})\mathcal{F}_J(\gamma)]$, where

$$\mathcal{F}_I(\gamma) = \frac{2\exp(-\gamma d_{I,J}^2)}{I\sqrt{2\pi}}\int_0^{+\infty}\frac{\exp(-x^2/2)\hat{\mathcal{F}}_I(x)}{\sum_{p=1}^{I/2}g_p\cosh\big(\sqrt{2\gamma}(2p-1)xd_{I,J}\big)}\mathrm{d}x, \qquad \text{(A.6)}$$

and $\hat{\mathcal{F}}_I(x) = \sum_{p=1}^{I/2}\sum_{l=1}^{I/2}g_l g_p\Big(4(2l-1)^2 d_{I,J}^2\cosh\big(\sqrt{2\gamma}(2l-1)xd_{I,J}\big)\cosh\big(\sqrt{2\gamma}(2p-1)xd_{I,J}\big)-4(2l-1)(2p-1)d_{I,J}^2\sinh\big(\sqrt{2\gamma}(2l-1)xd_{I,J}\big)\sinh\big(\sqrt{2\gamma}(2p-1)xd_{I,J}\big)\Big)$.

Taking partial derivatives of $\mathrm{LLF}_{I,k}$, we can show that

$$\frac{\partial^2\mathrm{LLF}_{I,k}}{\partial\varphi\partial\alpha} = \frac{\sum_{p=1}^{I/2}\sum_{l=1}^{I/2}g_l g_p\Im\{r_k e^{-j\varphi}\}\Big(\beta_1(\Re\{r_k e^{-j\varphi}\})+\beta_2(\Re\{r_k e^{-j\varphi}\})-\beta_3(\Re\{r_k e^{-j\varphi}\})\Big)}{\Big(\delta_I(\Re\{r_k e^{-j\varphi}\})\Big)^2}, \qquad \text{(A.7)}$$

where

$$\begin{cases} \beta_1(\Re\{r_k e^{-j\varphi}\}) = \big(\frac{2\alpha d_{I,J}^2 u_l}{\sigma^2}[(2p-1)^2-(2l-1)^2]+\frac{1}{\alpha}\big)\sinh(u_l\Re\{r_k e^{-j\varphi}\}) \\ \qquad\qquad\qquad \times\cosh(u_p\Re\{r_k e^{-j\varphi}\}), \\ \beta_2(\Re\{r_k e^{-j\varphi}\}) = \frac{u_l^2}{\alpha}\Re\{r_k e^{-j\varphi}\}\cosh(u_l\Re\{r_k e^{-j\varphi}\})\cosh(u_p\Re\{r_k e^{-j\varphi}\}), \\ \beta_3(\Re\{r_k e^{-j\varphi}\}) = \frac{u_l u_p}{\alpha}\Re\{r_k e^{-j\varphi}\}\sinh(u_l\Re\{r_k e^{-j\varphi}\})\sinh(u_p\Re\{r_k e^{-j\varphi}\}). \end{cases} \tag{A.8}$$

Taking expectation and changing variables similar to the proof of (A.4), we have $\mathbb{E}[\frac{\partial^2 \mathrm{LLF}_{I,k}}{\partial\varphi\partial\alpha}]=0$ since $\delta_J(y)$ is an even function of y and $\frac{2\exp\left(-\frac{\alpha^2 d_{I,J}^2}{\sigma^2}\right)}{J\sqrt{\pi\sigma^2}}\int_{-\infty}^{+\infty} y\exp(-\frac{y^2}{\sigma^2})\delta_J(y)\mathrm{d}y$ $=0$. In addition, it is easy to show that $\mathbb{E}[\frac{\partial^2\mathcal{C}}{\partial\varphi\partial\alpha}]=0$ and hence $\mathcal{I}_{1,2}=0$. Similarly, one can derive $\mathcal{I}_{2,1}=\mathcal{I}_{3,2}=\mathcal{I}_{2,3}=0$.

In order to find $\mathcal{I}_{1,1}$, we take the second derivative of $\mathrm{LLF}_{I,k}$ with respect to α, which is given by

$$\frac{\partial^2\mathrm{LLF}_{I,k}}{\partial\alpha^2}=\frac{\sum_{p=1}^{I/2}\sum_{l=1}^{I/2}\frac{g_l g_p d_{I,J}^2}{\sigma^2}\Big(\delta_{1,\alpha}(\Re\{r_k e^{-j\varphi}\})+\delta_{2,\alpha}(\Re\{r_k e^{-j\varphi}\})-\delta_{3,\alpha}(\Re\{r_k e^{-j\varphi}\})\Big)}{\big(\delta_I(\Re\{r_k e^{-j\varphi}\})\big)^2}, \tag{A.9}$$

where

$$\begin{cases} \delta_{1,\alpha}(\Re\{r_k e^{-j\varphi}\}) = 4u_l\big((2p-1)^2-(2l-1)^2\big)\Re\{r_k e^{-j\varphi}\}\sinh(u_l\Re\{r_k e^{-j\varphi}\}) \\ \qquad\qquad\qquad \times\cosh(u_p\Re\{r_k e^{-j\varphi}\}), \\ \delta_{2,\alpha}(\Re\{r_k e^{-j\varphi}\}) = \Big(2[(2l-1)^2-1]\big(\frac{2d_{I,J}^2\alpha^2}{\sigma^2}[(2l-1)^2-(2p-1)^2]-1\big) \\ \qquad\qquad\qquad +\frac{4(2l-1)^2}{\sigma^2}\Re^2\{r_k e^{-j\varphi}\}\Big)\cosh(u_l\Re\{r_k e^{-j\varphi}\})\cosh(u_p\Re\{r_k e^{-j\varphi}\}), \\ \delta_{3,\alpha}(\Re\{r_k e^{-j\varphi}\}) = \frac{4(2l-1)(2p-1)}{\sigma^2}\Re^2\{r_k e^{-j\varphi}\}\sinh(u_l\Re\{r_k e^{-j\varphi}\})\sinh(u_p\Re\{r_k e^{-j\varphi}\}). \end{cases} \tag{A.10}$$

After taking expectation and changing variables, we derive

$$\mathbb{E}\left[\frac{\partial^2\mathrm{LLF}_{I,k}}{\partial\alpha^2}\right]=-\mathcal{J}_{3,I}+\frac{2\exp\left(-\frac{\alpha^2 d_{I,J}^2}{\sigma^2}\right)}{I\sqrt{\pi\sigma^2}}\int_{-\infty}^{+\infty}\frac{\exp(-\frac{x^2}{\sigma^2})\tilde{\mathcal{G}}_I(x)}{\delta_I(x)}\mathrm{d}x, \tag{A.11}$$

where $\tilde{\mathcal{G}}_I(x) = \sum_{p=1}^{I/2}\sum_{l=1}^{I/2}\frac{g_l g_p d_{I,J}^2}{\sigma^2}\Big(\delta_{1,\alpha}(x)+\delta_{2,\alpha}(x)-\delta_{3,\alpha}(x)+2[(2l-1)^2-1]\cosh(u_l x)$ $\cosh(u_p x)\Big)$ and $\mathcal{J}_{3,I} = \frac{4d_{I,J}^2\exp\left(-\frac{\alpha^2 d_{I,J}^2}{\sigma^2}\right)}{\sigma^2 I\sqrt{\pi\sigma^2}}\int_{-\infty}^{+\infty}\exp(-\frac{x^2}{\sigma^2})\sum_{l=1}^{I/2}[(2l-1)^2-1]g_l\cosh(u_l x)\mathrm{d}x$. We can show that $\mathcal{J}_{3,I} = \frac{2(I^2-4)}{\sigma^2(I^2+J^2-2)}$. Furthermore, we can show that $\mathbb{E}[\frac{\partial^2\mathcal{C}}{\partial\alpha^2}] = -\frac{12K}{\sigma^2(I^2+J^2-2)}$. Using (A.11) and after some manipulations, we have $\mathcal{I}_{1,1} = \frac{2K}{\sigma^2}[1 - \frac{1}{2}\mathcal{G}_I(\gamma) - \frac{1}{2}\mathcal{G}_J(\gamma)]$, where

$$\mathcal{G}_I(\gamma) = \frac{4\exp(-\gamma d_{I,J}^2)}{I\sqrt{2\pi}}\int_0^{+\infty}\frac{\exp(-x^2/2)\hat{\mathcal{G}}_I(x)}{\sum_{p=1}^{I/2} g_p\cosh\left(\sqrt{2\gamma}(2p-1)x d_{I,J}\right)}\mathrm{d}x, \quad (A.12)$$

and $\hat{\mathcal{G}}_I(x) = \sum_{p=1}^{I/2}\sum_{l=1}^{I/2} 4d_{I,J}^2 g_l g_p\Big(\big(0.5(2l-1)^2x^2+\gamma d_{I,J}^2[(2l-1)^2-1][(2l-1)^2-(2p-1)^2]\big)\cosh\left(\sqrt{2\gamma}(2l-1)x d_{I,J}\right)\cosh\left(\sqrt{2\gamma}(2p-1)x d_{I,J}\right) - \sqrt{2\gamma}x d_{I,J}(2l-1)[(2l-1)^2 - (2p-1)^2]\sinh\left(\sqrt{2\gamma}(2l-1)x d_{I,J}\right)\cosh\left(\sqrt{2\gamma}(2p-1)x d_{I,J}\right) - \frac{(2l-1)(2p-1)}{2}x^2\sinh\left(\sqrt{2\gamma}(2l-1)x d_{I,J}\right)\sinh\left(\sqrt{2\gamma}(2p-1)x d_{I,J}\right)\Big)$.

In order to derive $\mathcal{I}_{1,3}$, we take partial derivatives of $\mathrm{LLF}_{I,k}$ which is given by

$$\frac{\partial^2\mathrm{LLF}_{I,k}}{\partial\sigma^2\partial\alpha} = \frac{\sum_{p=1}^{I/2}\sum_{l=1}^{I/2}\frac{g_l g_p d_{I,J}}{\sigma^4}\Big(\mu_1(\Re\{r_k e^{-j\varphi}\}) + \mu_2(\Re\{r_k e^{-j\varphi}\}) + \mu_3(\Re\{r_k e^{-j\varphi}\})\Big)}{\big(\delta_I(\Re\{r_k e^{-j\varphi}\})\big)^2}, \quad (A.13)$$

where

$$\begin{cases} \mu_1(\Re\{r_k e^{-j\varphi}\}) = \Re\{r_k e^{-j\varphi}\}\Big(3u_l d_{I,J}\alpha[(2l-1)^2-(2p-1)^2] - 2(2l-1)\Big) \\ \qquad\times\sinh(u_l\Re\{r_k e^{-j\varphi}\})\cosh(u_p\Re\{r_k e^{-j\varphi}\}), \\ \mu_2(\Re\{r_k e^{-j\varphi}\}) = \Big(2d_{I,J}\alpha[(2l-1)^2-1]\big(\frac{d_{I,J}^2\alpha^2}{\sigma^2}[(2p-1)^2-(2l-1)^2]+1\big) \\ \qquad - \frac{u_l^2\sigma^2}{d_{I,J}\alpha}\Re^2\{r_k e^{-j\varphi}\}\Big)\cosh(u_l\Re\{r_k e^{-j\varphi}\})\cosh(u_p\Re\{r_k e^{-j\varphi}\}), \\ \mu_3(\Re\{r_k e^{-j\varphi}\}) = \frac{u_l u_p\sigma^2}{d_{I,J}\alpha}\Re^2\{r_k e^{-j\varphi}\}\sinh(u_l\Re\{r_k e^{-j\varphi}\})\sinh(u_p\Re\{r_k e^{-j\varphi}\}). \end{cases} \quad (A.14)$$

Taking expectation and changing variables, we obtain

$$\mathbb{E}\left[\frac{\partial^2\mathrm{LLF}_{I,k}}{\partial\sigma^2\partial\alpha}\right] = \mathcal{J}_{4,I} - \mathcal{J}_{5,I} + \frac{2\exp\left(-\frac{\alpha^2 d_{I,J}^2}{\sigma^2}\right)}{I\sqrt{\pi\sigma^2}}\int_{-\infty}^{+\infty}\frac{\exp(-\frac{x^2}{\sigma^2})\tilde{\mathcal{H}}_I(x)}{\delta_I(x)}\mathrm{d}x, \quad (A.15)$$

where $\tilde{\mathcal{H}}_I(x) = \sum_{p=1}^{I/2}\sum_{l=1}^{I/2} \frac{g_l g_p d_{I,J}}{\sigma^4}\Big(\mu_1(x)+\mu_2(x)+\mu_3(x)-2d_{I,J}\alpha[(2l-1)^2-1]\cosh(u_l x)$ $\cosh(u_p x)+2(2l-1)x\sinh(u_l x)\cosh(u_p x)\Big)$, $\mathcal{J}_{4,I} = \frac{4d_{I,J}^2\alpha\exp\left(-\frac{\alpha^2 d_{I,J}^2}{\sigma^2}\right)}{\sigma^4 I\sqrt{\pi\sigma^2}}\int_{-\infty}^{+\infty}\exp(-\frac{x^2}{\sigma^2})\sum_{l=1}^{I/2}[(2l-1)^2-1]g_l\cosh(u_l x)\mathrm{d}x$, and $\mathcal{J}_{5,I} = \frac{4d_{I,J}\exp\left(-\frac{\alpha^2 d_{I,J}^2}{\sigma^2}\right)}{\sigma^4 I\sqrt{\pi\sigma^2}}\int_{-\infty}^{+\infty}\exp(-\frac{x^2}{\sigma^2})\sum_{l=1}^{I/2}(2l-1)g_l x\sinh(u_l x)\mathrm{d}x$. We can show that $\mathcal{J}_{4,I} = \frac{2\alpha}{\sigma^4}\frac{I^2-4}{I^2+J^2-2}$ and $\mathcal{J}_{5,I} = \frac{2\alpha}{\sigma^4}\frac{I^2-1}{I^2+J^2-2}$. Also, we have $\mathbb{E}[\frac{\partial^2\mathcal{C}}{\partial\sigma^2\partial\alpha}] = \frac{4K\alpha}{\sigma^4}\frac{3}{I^2+J^2-2}$. Using (A.15) and after some manipulations, we derive $\mathcal{I}_{1,3} = \mathcal{I}_{3,1} = \frac{2K\alpha}{\sigma^4}[\frac{1}{2}\mathcal{H}_I(\gamma)+\frac{1}{2}\mathcal{H}_J(\gamma)]$, where

$$\mathcal{H}_I(\gamma) = \frac{4\exp(-\gamma d_{I,J}^2)}{I\sqrt{2\pi}}\int_0^{+\infty}\frac{\exp(-x^2/2)\hat{\mathcal{H}}_I(x)}{\sum_{p=1}^{I/2} g_p\cosh\left(\sqrt{2\gamma}(2p-1)xd_{I,J}\right)}\mathrm{d}x, \qquad \text{(A.16)}$$

and $\hat{\mathcal{H}}_I(x) = \sum_{p=1}^{I/2}\sum_{l=1}^{I/2} 2d_{I,J}^2 g_l g_p\Big(\big((2l-1)^2x^2+\gamma d_{I,J}^2[(2l-1)^2-1][(2l-1)^2-(2p-1)^2]\big)\cosh\left(\sqrt{2\gamma}(2l-1)xd_{I,J}\right)\cosh\left(\sqrt{2\gamma}(2p-1)xd_{I,J}\right)-1.5\sqrt{2\gamma}xd_{I,J}(2l-1)[(2l-1)^2-(2p-1)^2]\sinh\left(\sqrt{2\gamma}(2l-1)xd_{I,J}\right)\cosh\left(\sqrt{2\gamma}(2p-1)xd_{I,J}\right)-(2l-1)(2p-1)x^2\sinh\left(\sqrt{2\gamma}(2l-1)xd_{I,J}\right)\sinh\left(\sqrt{2\gamma}(2p-1)xd_{I,J}\right)\Big)$.

In order to find $\mathcal{I}_{3,3}$, we take the second derivative of $\mathrm{LLF}_{I,k}$ with respect to σ^2 which is given by

$$\frac{\partial^2\mathrm{LLF}_{I,k}}{\partial\sigma^4} = \frac{\sum_{p=1}^{I/2}\sum_{l=1}^{I/2}\frac{g_l g_p\alpha d_{I,J}}{\sigma^6}\Big(\delta_{1,\sigma^2}(\Re\{r_k e^{-j\varphi}\})+\delta_{2,\sigma^2}(\Re\{r_k e^{-j\varphi}\})-\delta_{3,\sigma^2}(\Re\{r_k e^{-j\varphi}\})\Big)}{\big(\delta_I(\Re\{r_k e^{-j\varphi}\})\big)^2}, \qquad \text{(A.17)}$$

where

$$\begin{cases}\delta_{1,\sigma^2}(\Re\{r_k e^{-j\varphi}\}) = \Re\{r_k e^{-j\varphi}\}\Big(-2u_l d_{I,J}\alpha[(2l-1)^2-(2p-1)^2]+4(2l-1)\Big) \\ \qquad\qquad \times\sinh(u_l\Re\{r_k e^{-j\varphi}\})\cosh(u_p\Re\{r_k e^{-j\varphi}\}), \\ \delta_{2,\sigma^2}(\Re\{r_k e^{-j\varphi}\}) = \Big(d_{I,J}\alpha[(2l-1)^2-1]\big(\frac{d_{I,J}^2\alpha^2}{\sigma^2}[(2l-1)^2-(2p-1)^2]-2\big) \\ \qquad\qquad +\frac{u_l^2\sigma^2}{d_{I,J}\alpha}\Re^2\{r_k e^{-j\varphi}\}\Big)\cosh(u_l\Re\{r_k e^{-j\varphi}\})\cosh(u_p\Re\{r_k e^{-j\varphi}\}), \\ \delta_{3,\sigma^2}(\Re\{r_k e^{-j\varphi}\}) = \frac{u_l u_p\sigma^2}{d_{I,J}\alpha}\Re^2\{r_k e^{-j\varphi}\}\sinh(u_l\Re\{r_k e^{-j\varphi}\})\sinh(u_p\Re\{r_k e^{-j\varphi}\}).\end{cases} \qquad \text{(A.18)}$$

Taking expectation and changing variables, we have

$$\mathbb{E}\left[\frac{\partial^2 \mathrm{LLF}_{I,k}}{\partial\sigma^4}\right] = \frac{\alpha}{\sigma^2}(-\mathcal{J}_{4,I} + 2\mathcal{J}_{5,I}) + \frac{2\exp\left(-\frac{\alpha^2 d_{I,J}^2}{\sigma^2}\right)}{I\sqrt{\pi\sigma^2}} \int_{-\infty}^{+\infty} \frac{\exp(-\frac{x^2}{\sigma^2})\tilde{\mathcal{K}}_I(x)}{\delta_I(x)}\mathrm{d}x, \tag{A.19}$$

where $\tilde{\mathcal{K}}_I(x) = \sum_{p=1}^{I/2}\sum_{l=1}^{I/2} \frac{g_l g_p d_{I,J}\alpha}{\sigma^6}\Big(\delta_{1,\sigma^2}(x) + \delta_{2,\sigma^2}(x) - \delta_{3,\sigma^2}(x) + 2d_{I,J}\alpha[(2l-1)^2 - 1]\cosh(u_l x)\cosh(u_p x) - 4(2l-1)x\sinh(u_l x)\cosh(u_p x)\Big)$. In addition, we have $\mathbb{E}[\frac{\partial^2 \mathcal{C}}{\partial\sigma^4}] = -\big(\frac{K}{\sigma^4} + \frac{2k\alpha^2}{\sigma^6}(\frac{3}{I^2+J^2-2} + 1)\big)$. Using (A.19) and after some manipulations, we obtain $\mathcal{I}_{3,3} = \frac{K}{\sigma^4} - \frac{K\alpha^2}{\sigma^6}[\mathcal{K}_I(\gamma) + \mathcal{K}_J(\gamma)]$, where

$$\mathcal{K}_I(\gamma) = \frac{4\exp(-\gamma d_{I,J}^2)}{I\sqrt{2\pi}} \int_0^{+\infty} \frac{\exp(-x^2/2)\hat{\mathcal{K}}_I(x)}{\sum_{p=1}^{I/2} g_p \cosh\left(\sqrt{2\gamma}(2p-1)x d_{I,J}\right)}\mathrm{d}x, \tag{A.20}$$

and $\hat{\mathcal{K}}_I(x) = \sum_{p=1}^{I/2}\sum_{l=1}^{I/2} d_{I,J}^2 g_l g_p \Big(\big(2(2l-1)^2 x^2 + \gamma d_{I,J}^2[(2l-1)^2 - 1][(2l-1)^2 - (2p-1)^2]\big)\cosh\left(\sqrt{2\gamma}(2l-1)x d_{I,J}\right)\cosh\left(\sqrt{2\gamma}(2p-1)x d_{I,J}\right) - 2\sqrt{2\gamma}x d_{I,J}(2l-1)[(2l-1)^2 - (2p-1)^2]\sinh\left(\sqrt{2\gamma}(2l-1)x d_{I,J}\right)\cosh\left(\sqrt{2\gamma}(2p-1)x d_{I,J}\right) - 2(2l-1)(2p-1)x^2\sinh\left(\sqrt{2\gamma}(2l-1)x d_{I,J}\right)\sinh\left(\sqrt{2\gamma}(2p-1)x d_{I,J}\right)\Big)$. Substituting $\mathcal{I}_{b,c}$ for $b, c = 1,\ 2,$ and 3 into (2.30), (2.31) is obtained and the proof is complete.

Chapter 3

Conclusions and Future Work

3.1 Conclusions

Recognizing the modulation scheme of the received signal without having knowledge of the propagation environment is an important step before demodulation in various military and commercial applications. In multi-path fading environments, the problem becomes more challenging. In addition, the classification performance improves by using multiple antenna receivers. The spatial diversity achieved by using multiple independent replicas of the transmitted symbol mitigates the fading effects of the environment and yields improvement in probability of correct detection. This thesis focuses on the LB algorithms of blind MC for a multiple antenna receivers configuration.

The expressions of theoretical performance analysis are useful tools to guide the process of designing communication systems. If deriving the exact analytical expressions is not tractable, one can resort to proper bounds, *e.g.,* the CRLBs of the unknown parameters give us an idea on how accurately the unbiased estimates are performing.

Firstly, we have proposed a new WS-based algorithm for a SIMO configuration assuming amplitude, phase, and noise variance to be unknown. The conditional LFs of the received signal under the modulation scheme and unknown quantities were derived. Then the unconditional LFs were computed by using the state-of-the-art NDA estimates for the unknown parameters and taking expectation over the transmitted symbols. It is demonstrated that our proposed algorithm outperformed the extended algorithm existing in the literature. An upper bound on the performance of any MC algorithms and another bound on the QHRLT-based algorithms were provided. The former, ALRT-UB, was obtained to evaluate the performance loss of MC algorithms when compared to the ideal case, *i.e.,* no unknown parameter. The latter, QHLRT-UB, provided a bound on QHLRT-based algorithms employing NDA and unbiased estimates of the unknown parameters. Numerical results showed that the proposed algorithm outperformed the existing algorithm significantly and its performance was close to the derived upper bounds.

Secondly, the exact expressions of the CRLBs of amplitude, phase, noise variance, and SNR for general rectangular $I \times J$-QAM signals were obtained. Furthermore, we derived the asymptotic CRLBs for high SNR regime. Numerical results verified the accuracy of our analysis and demonstrated that the results available in the literature were special cases of our results.

Finally, the proposed algorithm in this thesis can be employed in modern intelligent radios equipped with multiple antenna receivers. The derived expressions of performance analysis can be used to guide practical systems design involving estimation of the unknown parameters and is not limited to modulation classification.

As an example, some parameters such as SNR, the number of receiving antennas, and the number of observed symbols may be optimized to have an appropriate trade-off between system performance and computational complexity determined by the quality-of-service demanded by the application.

3.2 Future Work

There are still many rooms for developing future work on the LB-MC algorithms in multi-path fading environments. The work presented in this thesis may be developed further in many ways.

The work of Section 2.3.2, the proposed MC algorithm for multiple antennas, may be developed further in the following ways. In the development presented in Section 2.3.2, we assumed that the receiver side has no knowledge of the instantaneous C-SI and the noise variances. If the receiver had accurate information of the CSI and variances, it might be tractable to analyze the exact analytical expression of the probability of correct classification and further employ it to maximize the performance by optimizing some parameters such as beamforming coefficients. Furthermore, we investigate the LB-MC algorithms only for a SIMO configuration. It would be more useful to generalize the problem to multiple-input-multiple-output (MIMO) or cooperative diversity networks with arbitrary number of relays. Also, it is useful and interesting to consider the problem of joint detection and MC. For this scenario, one will find the unknown modulation scheme and then starts detecting the symbols. Bit-error-rate (BER) of the received signal could be used as a new performance measure which we are interested to minimize.

The work of Section 2.4, upper bound analysis of QHLRT, may be also studied further. We have already obtained the exact CRLBs of rectangular QAM for SISO. However, to the best of our knowledge, there has been no work on the CRLBs for SIMO where there are multiple unknown parameter vectors. This could be an interesting problem as a possible future work. Another possibility is to consider more unknown parameters such as carrier frequency offset or timing offset.

Bibliography

[1] O. A. Dobre, A. Abdi, Y. Bar-Ness, and W. Su, "Survey of automatic modulation classification techniques: classical approaches and new trends," *IET Commun.*, vol. 1, pp. 137–156, Apr. 2007.

[2] J. L. Xu, W. Su, and M. Zhou, "Likelihood–ratio approaches to automatic modulation classification," *IEEE Trans. Systems, Man, and Cybernetics–Part C*, vol. 41, pp. 455–469, July 2011.

[3] C. Y. Huang and A. Polydoros, "Advanced methods for digital quadrature and offset modulation classification," in *Proc. IEEE MILCOM*, vol. 2, pp. 841–845, Oct. 1988.

[4] C. Y. Hwang and A. Polydoros, "Likelihood methods for MPSK modulation classification," *IEEE Trans. Commun.*, vol. 43, pp. 1493–1504, Apr. 1995.

[5] A. Abdi, O. A. Dobre, R. Choudhry, Y. Bar-Ness, and W. Su, "Modulation classification in fading channels using antenna arrays," in *Proc. IEEE MILCOM*, vol. 1, pp. 211–217, Nov. 2004.

[6] O. A. Dobre and F. Hameed, "Likelihood–based algorithms for linear digital modulation classification in fading channels," in *Proc. IEEE CCECE*, pp. 1347–1350, May 2006.

[7] F. Hameed, O. A. Dobre, and D. C. Popescu, "On the likelihood–based approach to modulation classification," *IEEE Trans. Wireless Commun.*, vol. 8, pp. 5884–5892, Dec. 2009.

[8] M. Derakhtian, A. A. Tadaion, and S. Gazor, "Modulation classification of linearly modulated signals in slow flat fading channels," *IET Signal Processing*, vol. 5, pp. 443–450, Aug. 2011.

[9] J. L. Xu, W. Su, and M. Zhou, "Distributed automatic modulation classification with multiple sensors," *IEEE Sensors Journal*, vol. 10, pp. 1779–1785, Nov. 2010.

[10] P. Panagiotou, A. Anastasopoulos, and A. Polydoros, "Likelihood ratio tests for modulation classification," in *Proc. IEEE MILCOM*, vol. 2, pp. 670–674, 2000.

[11] S. Xi and H. C. Wu, "Robust automatic modulation classification using cumulant features in the presence of fading channels," in *Proc. IEEE WCNC*, vol. 4, pp. 2094–2099, 2006.

[12] B. Ramkumar, T. Bose, and M. S. Radenkovic, "Robust multiuser automatic modulation classifier for multipath fading channels," in *Proc. IEEE DySPAN*, pp. 1–10, Apr. 2010.

[13] W. Dai, Y. Wang, and J. Wang, "Joint power estimation and modulation classification using second- and higher statistics," in *Proc. IEEE WCNC*, vol. 1, pp. 155–158, 2002.

[14] U. Mengali and A. N. D'Andrea, *Synchronization Techniques for Digital Receivers*, New York: Plenum, 1997.

[15] D. R. Pauluzzi and N. C. Beaulieu, "A comparison of SNR estimation techniques for the AWGN channel," *IEEE Trans. Commun.*, vol. 48, pp. 1681–1691, Oct. 2000.

[16] W. Wei and J. M. Mendel, "Maximum–likelihood classification for digital amplitude-phase modulations," *IEEE Trans. Commun.*, vol. 48, pp. 189–193, Feb. 2000.

[17] P. Campisi, G. Panci, S. Colonnese, and G. Scarano, "Blind phase recovery for QAM communication systems," *IEEE Trans. Signal Process.*, vol. 53, pp. 1348–1358, Apr. 2005.

[18] A. Stéphenne, F. Bellili, and S. Affes, "Moment-based SNR estimation over linearly-modulated wireless SIMO channels," *IEEE Trans. Wireless Commun.*, vol. 9, pp. 714–722, Feb. 2010.

[19] F. Bellili, A. Stéphenne, and S. Affes, "Cramér-Rao lower bounds for non-data-aided SNR estimates of square QAM modulated transmissions," *IEEE Trans. Commun.*, vol. 58, pp. 3211–3218, Nov. 2010.

[20] F. Bellili, N. Atitallah, S. Affes, and A. Stéphenne, "Cramér-Rao lower bounds for frequency and phase non-data-aided estimation from arbitrary square

QAM-modulated signals," *IEEE Trans. Signal Process.*, vol. 58, pp. 4517–4525, Sep. 2010.

[21] S. M. Kay, *Fundamentals of Statistical Signal Processing, Estimation Theory.* Upper Saddle River, NJ: Prentice Hall, 1993.

[22] H. L. Van Trees, *Detection, Estimation, and Modulation Theory.* New York: Wiley, 2001.

[23] E. E. Azzouz and A. K. Nandi, *Automatic Modulation Recognition of Communication Signals.* Norwell, MA: Kulwer, 1996.

[24] S.-Z. Hsue and S. S. Soliman, "Automatic modulation classification using zero crossing," in *Proc. Inst. Elect. Eng.*, vol. 137, pp. 459–464, 1990.

[25] K. C. Ho, W. Prokopiw, and Y. T. Chan, "Modulation identification by the wavelet transform," in *Proc. IEEE MILCOM.*, vol. 2, pp. 886–890, 1995.

[26] K. C. Ho, W. Prokopiw, and Y. T. Chan, "Modulation identification of digital signals by the wavelet transform," *IEE Proc., Radar, Sonar Navig.*, vol. 147, pp. 169–176, 2000.

[27] L. Hong and K. C. Ho, "Identification of digital modulation types using the wavelet transform," in *Proc. IEEE MILCOM.*, vol. 1, pp. 427–431, 1999.

[28] A. Swami and B. M. Sadler, "Hierarchical digital modulation classification using cumulants," *IEEE Trans. Commun.*, vol. 48, pp. 416–429, Mar. 2000.

[29] C. Martret and D. M. Boiteau, "Modulation classification by means of different orders statistical moments," in *Proc. IEEE MILCOM.*, vol. 3, pp. 1387–1391, 1997.

[30] O. A. Dobre, Y. Bar-Ness, and W. Su, "Higher-order cyclic cumulants for high order modulation classification," in *Proc. IEEE MILCOM.*, vol. 1, pp. 112–117, 2003.

[31] O. A. Dobre, Y. Bar-Ness, and W. Su, "Robust QAM modulation classification algorithm based on cyclic cumulants," in *Proc. WCNC.*, vol. 2, pp. 745–748, 2004.

[32] W. Wei and J. M. Mendel, "A fuzzy logic method for modulation classification in nonideal environments," *IEEE Trans. Fuzzy Syst.*, vol. 7, pp. 333–344, June 1999.

[33] B. G. Mobasseri, "Constellation shape as a robust signature for digital modulation recognition," in *Proc. IEEE MILCOM.*, vol. 1, pp. 442–446, 1999.

[34] U. Mengali and M. Morelli, "Data-aided frequency estimation for burst digital transmission," *IEEE Trans. Commun.*, vol. 45, pp. 23–25, Jan. 1997.

[35] R. López-Valcarce and C. Mosquera, "Sixth-order statistics-based non-data-aided SNR estimation," *IEEE Commun. Lett.*, vol. 11, pp. 351–353, Apr. 2007.

[36] C. Mosquera, S. Scalise, and R. López-Valcarce, "Non-data-aided symbol rate estimation of linearly modulated signals," *IEEE Trans. Signal Process.*, vol. 56, pp. 664–674, Feb. 2008.

[37] M. J. Schervish, *Theroy of Statistics.* New York: Springer, 1995.